Article:
Mueller, P, Langone, A, Patacci, M et al. (2018) Detrital signatures of impending collision: The deep-water record of the Upper cretaceous Bordighera Sandstone and its basal complex (Ligurian Alps, Italy). Sedimentary Geology, 377. pp. 147-161. ISSN: 0037-0738

https://doi.org/10.1016/j.sedgeo.2018.10.002

Detrital signatures of impending collision: The deep-water record of the Upper Cretaceous Bordighera Sandstone and its basal complex (Ligurian Alps, Italy)

Pierre Mueller[1]*, Antonio Langone[2], Marco Patacci[3], Andrea Di Giulio[1]

[1]. Dipartimento di Scienze della Terra e dell'Ambiente, Università di Pavia, Pavia, Italy.

[2]. CNR – Istituto di Geoscienze e Georisorse, Unità di Pavia, Via Ferrata 1, 27100 Pavia, Italy

[3]. Turbidites Research Group, School of Earth and Environment, University of Leeds, Leeds, LS2 9JT, UK.

*Corresponding author; Email-address: pierre.mueller01@universitadipavia.it (P. Mueller)

Abstract

Despite intensive research efforts and significant advances in the understanding of subduction and obduction processes that affected several units which at the present day compose the Western Alps, the paleogeographic evolution of the Alpine Tethys represents a debated topic in Alpine geology. The role of the opposing continental margins (passive European margin and active Adriatic margin) as source regions for Cretaceous siliciclastic turbidites bordering the convergent system remains disputed. To address this question along the Ligurian Alps transect, a multi-proxy provenance analysis is applied to the two terrigenous superimposed units (Hauterivian-Campanian San Bartolomeo Fm. and Campanian-Maastrichtian Bordighera Sandstone) of the San Remo-Monte Saccarello Unit of the Western Ligurian Flysch complex. Petrographic analyses characterize the basal San Bartolomeo Fm. as quartz-rich mature sandstones. By contrast, the overlying Bordighera Sandstone represents texturally and compositionally immature first-cycle arkosic arenites. This change records the evolution of the sediment provenance from a stable craton into a continental basement uplift setting, reflecting erosion of granitoid plutons and the low-grade metamorphic basement. Geochronological data (U-Pb detrital zircon ages) indicate that virtually the same source terranes provided the source for both formations. The detrital age spectra display age peaks are compatible with well-documented magmatic and metamorphic pulses that affected the Southern Variscides in the Paleo-European margin. The strong

affinity of clastic detritus with the Paleo-European margin basement rocks underlines the importance of the lower plate passive continental margin in supplying sand-rich turbidite systems prior to the arrival of the passive margin in the subduction zone.

Keywords: Sandstone provenance; (U-Pb) detrital zircon chronology; Piedmont-Ligurian ocean; Tethyan continental margins; subduction; impending collision.

1 Introduction

The geodynamic evolution of the Western Tethys during the Alpine subduction remains debated, with various models emphasizing on opposite subduction polarities and the presence of continental fragments and their role in the context of the pre-collisional geodynamic evolution of the Piedmont-Ligurian oceanic domain (e.g., Froitzheim and Manatschal, 1996; Dal-Piaz et al., 2003; Froitzheim et al., 2008; Molli, 2008; Alvarez and Shimabukuro, 2009; Viti et al., 2009; Handy et al., 2010, 2014; Marroni et al., 2010; Molli and Malavieleille, 2011; Decarlis et al., 2013; Malusà et al., 2015; Lin et al., 2018). Owing to crustal shortening and subduction, oceanic units became displaced, so that the reconstruction of their original positions remains uncertain. To this end, Upper Cretaceous to Paleogene turbiditic sequences scraped off in front of the Alpine subduction zone provide key evidence for Alpine convergence, predating continental collision after the closure of the Piedmont-Ligurian ocean in the early Cenozoic (e.g., Lanteaume, 1962; Sagri and Marri, 1980; Caron et al., 1981). The detrital signatures of these pre-collisional sequences that crop out along the entire Alpine belt allow insights into the plate-tectonic setting of the continental areas bordering the ocean and providing the source of the clastic detritus (e.g., Valloni and Zuffa, 1984; Fontana et al., 1994; Bracciali et al., 2014).

According to classical provenance models, the relative proportions of distinct types of terrigenous sand grains mirror the nature of the parent rocks of the clastic detritus, and in turn also provide information of the geodynamic setting of source to sink systems (e.g., Dickinson and Suczek, 1979; Bhatia, 1983; Dickinson et al., 1983; Dickinson, 1985; Garzanti et al., 2007; 2014). Moreover, the relationship

between hinterland tectonics and associated sediment dispersal pathways towards the final depositional environments of the siliciclastic detritus can be reconstructed. Even though sandstone petrography depicts the most feasible link to reconstruct hinterland tectonics, the quantification of detrital components does not provide insights into the age of the parent rocks and the thermal history they underwent (Fedo et al., 2003; Andersen, 2005; Najman, 2006). Accordingly, additional data are required to pass from a generic definition of the source region to a paleogeographic picture where those areas are regionally constrained. Provenance studies increasingly highlight the advantage of combining sandstone petrography with geo-thermochronological analysis of detrital minerals and hence elaborate a ‘‘multi-proxy’’ source discrimination (e.g., Dunkl et al., 2001; Dickinson and Gehrels, 2009; Beltrán-Triviño et al., 2013; Bracciali et al., 2014; Di Giulio et al., 2017).

Here we apply this approach to the San Remo-Monte Saccarello Unit, the stratigraphically oldest and tectonically topmost unit of the Western Ligurian Flysch cropping out in NW Italy. The unit is interpreted to represent trench-fill successions that were scraped off from their oceanic substratum and became incorporated into the Alpine accretionary prism along the Ligurian Alps transect (Di Giulio, 1992). An integrated sediment provenance analysis that comprises modal framework analysis, detrital zircon U-Pb geochronology and the study of sediment dispersal patterns of the two terrigenous members of the unit is undertaken. The results validate the debated hypothesis that the detrital source was provided by the passive European continental margin approaching the subduction zone instead of the active Adriatic margin. Additionally, they show that activation of the studied deep marine clastic systems records the arrival of a passive continental margin in the subduction zone, immediately predating the transition from an oceanic subduction setting to that of a continental collision zone.

2 Background tectonics and stratigraphy

2.1 Tectonics

The study addresses the structurally topmost unit of the Cretaceous-Paleocene Western Ligurian Helminthoid Flysch Complex of the Ligurian Alps (Fig. 1). The Helminthoid Flysch Nappe represents the uppermost part of the Upper Penninic Nappe pile. During the late Eocene-early Oligocene the Helminthoid Flysch Units of the Ligurian Alps were thrusted over the more proximal domains of the European foreland and at the present day rest on the Mesozoic Dauphinois-Provençal succession (e.g., Vanossi et al., 1986; Di Giulio, 1992; Seno et al., 2005; Maino et al., 2015). They represent the accretionary wedge formed by the cover of the Piedmont-Ligurian ocean that was scraped off along the Ligurian Alps transect of the Alpine subduction system (Lanteaume, 1962; Vanossi et al., 1986; Di Giulio, 1992). The Western Ligurian Flysch Complex comprises four main subduction flysch units that from oldest to youngest are: the San Remo-Monte Saccarello Unit, the Moglio-Testico Unit, the Borghetto d´Arroscia Unit, and the Colla Domenica-Leverone Unit. These units are divided by southward dipping thrusts and are tectonically arranged in inverted chronostratigraphic order, with the oldest unit resting on top of the nappe pile, following the typical tectonic inversion of accretionary wedges (Di Giulio, 1992; Gasinski et al., 1997). The three lowermost and younger units underwent multi-phase ductile-brittle deformation, whereas the oldest and topmost San Remo-Monte Saccarello Unit is characterized by a rather simple structural setting, with relatively large-scale, open SW-verging kink folds (e.g., Di Giulio, 1992; Seno et al., 2005; Maino and Seno, 2016).

2.2 Stratigraphy

The San Remo-Monte Saccarello Unit consists of calcareous and mixed siliciclastic-calcareous successions that were deposited in abyssal environments in the Piedmont-Ligurian oceanic basin (Sagri, 1984; Di Giulio, 1992). This basin represents a branch of the Western Tethys that developed between the European and the Adria continental margins as a result of sequential rifting and spreading stages from early to late Jurassic (e.g., Marroni and Pandolfi, 2007 and references therein). The San Remo-Monte Saccarello Unit is divided in three lithostratigraphic units (Fig. 2A, B). The base of the unit is made up of the San Bartolomeo Formation, a succession of laterally extensive, thin-bedded and very

fine-grained turbidites. This unit is interpreted as representing the abyssal plain deposits which form the allochthonous "basal complex" of the overlying turbidites (Vanossi et al., 1986). Varicolored Mn-rich shales at the base of the unit are overlain by more sandy shales and thin-bedded turbiditic limestones with minor intercalations of fine-grained sandstones towards the top of the formation (Di Giulio and Galbiati, 1985). Based on foraminiferal faunas, the age of the San Bartolomeo Fm. can be constrained to late Hauterivian to Campanian (Cobianchi et al., 1991; Galbiati and Cobianchi, 1998). The San Bartolomeo Fm. reaches an overall thickness of 200 – 300 m (Giammarino et al., 2010) and is conformably superimposed by both the Bordighera Sandstone and the San Remo Flysch (Di Giulio, 1992). Owing to a scarcity of microfaunas, the depositional ages of these younger formations are not well defined but can be attributed to the Campanian-Maastrichtian (Di Giulio, 1992; Giammarino et al., 2010). The Bordighera Sandstone mainly consists of medium- to thick-bedded, microconglomeratic to medium-grained siliciclastic turbiditic beds and reaches a thickness of more than 250 m (Giammarino et al., 2010). A general south to north, proximal to distal facies trend defines the sand-rich turbidite system (Sagri, 1980; Mueller et al., 2017). The San Remo Flysch is primarily made up of medium- to thick-bedded, fine-grained calcareous turbiditic sediments and ranges in thickness between 100 m and 650 m (Giammarino et al., 2010). These formations are interpreted to have been deposited in an abyssal domain below the carbonate compensation depth, presumably in a trench environment (Sagri, 1980; Di Giulio, 1992).

3 Samples and methodology

The sampling strategy intended to provide full coverage of the vertical stratigraphic expression of the San Bartolomeo Fm. succession and of the Bordighera Sandstone turbidite system. Sample locations are illustrated in Fig. 2A. Twelve samples from the San Bartolomeo Fm. were acquired from outcrops located in immediate vicinity to the type locality in the Valle Argentina (Fig. 3A, B). Samples from two continuously exposed stratigraphic sections of the Bordighera Sandstones were selected: (i) nineteen samples from the Monte Frontè section (Fig. 3C), in the axial domain, and (ii) eleven samples from the

129 Cima di Velega section (Fig. 3D), representative of the more distal preserved part of the system (see
130 Mueller et al., 2017). The two sampled sections of the Bordighera Sandstones were selected because
131 they both include a stratigraphically conformable basal contact with the San Bartolomeo Formation.
132 Subsequently, thin-sections of 42 medium- to very fine-grained rock samples were prepared and
133 analyzed by optical microscopy.

134 Petrographic analysis was conducted by a standard point-counting at the optical microscope according
135 to guidelines provided by Di Giulio and Valloni (1992), following the Gazzi-Dickinson approach in order
136 to reduce bias in modal composition due to sample size effects (cf., Ingersoll et al., 1984; Dickinson,
137 1985). Modal analysis was performed by counting a minimum of 250 framework grains per thin-section
138 under both plane-parallel polarized and cross-polarized light. Framework parameters and full modal
139 analysis results are reported in Supplementary data file 1. The degree of grain roundness was
140 evaluated by visual comparison of the counted grains. Compositional maturity of sandstones was
141 appraised by calculating the maturity index (MI), i.e., the ratios of total quartz grains over the sum of
142 all feldspar grains and lithic fragments: MI = $\frac{Q}{(F+L)}$ (Pettijohn, 1975).

143 Sandstone petrography analysis was supplemented by U-Pb detrital zircon chronology (e.g., Fedo et
144 al., 2003; Andersen, 2005; Dickinson and Gehrels, 2009). Six samples for detrital zircon age
145 determinations were collected from stratigraphic intervals identical to those sampled for petrographic
146 analysis (see Fig. 2B). Of these, three samples from different stratigraphic intervals of the San
147 Bartolomeo Fm. were collected out of which only two yielded suitable quantities of detrital zircons.
148 The other three samples come from the Bordighera Sandstone, one from the medial Monte Frontè
149 section and two samples from the base and top of the more distal Cima di Velega section. The samples
150 were processed for heavy mineral and detrital zircon separation by grinding, hydrodynamic
151 procedures, magnetic isodynamic and heavy liquid separation (performed at the University of Padova).
152 Separated zircons were hand-picked, placed into epoxy resin and polished to expose the zircon cores.
153 For the purpose of revealing morphologies and internal structures of analyzed grains, micro-scale
154 cathodoluminescence imaging was performed at the University of Genova and ENI SpA Laboratories.

U-Pb detrital zircon ages were determined at the LA-ICP-MS lab at the CNR - Istituto di Geoscienze e Georisorse, Unità di Pavia, Italy. Analytical procedures of detrital zircon U-Pb age determinations and analytical setups are presented in Supplementary data file 2. Only U-Pb ages with a discordance smaller than 10% were considered as reliable ($^{206}Pb/^{238}U$ ratios for grains younger and $^{206}Pb/^{207}Pb$ data for grains older than 1.2 Ga; cf., Gehrels et al., 2009). Discordant data were rejected. U-Pb precision estimations referred to in the text and figures are reported as 2σ values. Probability density plots (PDPs) and kernel density estimated (KDEs) were plotted with the DensityPlotter 8.1 software (Vermeesch, 2012). Statistical evaluation of detrital zircon age spectra similarities was conducted utilizing the DZStats 2.2 software (Saylor and Sundell, 2016).

4 Results from modal framework analysis

4.1 Detrital petrology of the San Bartolomeo Formation (basal complex)

Average grain size of the analyzed samples of the San Bartolomeo Formation ranges from very fine to fine sand. Sorting is predominantly well to moderate (Fig. 4A-C). Grains are typically sub-rounded to rounded (Fig. 4B). Sandstone grains are relatively loosely packed, with an average content of intergranular constituents (matrix and cements) of ca. 19% of total rock volume. Quartz represents the dominant constituent of the basal complex sands. Among the quartz grains, monocrystalline quartz is the by far most abundant quartz component (mean Qm/Qp ratio: 6.14). Alkali feldspar proportions are higher than those of plagioclase (mean P/K-ratio: 0.48). Lithic fragments occur in very small quantities, with metamorphic fragments slightly dominating over volcanic and sedimentary rock fragments. The samples show high compositional maturity, with maturity index values ranging from 1.46 to 3.73 (mean MI = 2.32). Accessory constituents are micas, siliciclastic mudclasts and heavy minerals, with zircons representing the most widespread heavy mineral variety.

4.2 Detrital petrology of the Bordighera Sandstone

179 The mean grain size of the analyzed Bordighera Sandstone samples is medium sand, associated with a
180 poor degree of sorting. Framework grains are typically angular to sub-angular (Fig. 4D-F). Minor
181 occurrences of sub-rounded grains are generally limited to samples of the uppermost parts of the
182 stratigraphic sections. The samples are characterized by relatively loose packing as the average matrix
183 content is 10% of total rock volume (see also Fig. 4D, E). Among the main framework components,
184 detrital quartz grains make up the majority. Monocrystalline quartz dominates over polycrystalline
185 quartz varieties (mean Qm/Qp ratio: 1.92). Polycrystalline quartz varieties exhibit both straight and
186 sutured grain boundaries. Alkali feldspar concentrations exceed those of plagioclase (mean P/K-ratio:
187 0.56). Lithic fragments represent a recalculated average of 2%. Despite sedimentary, volcanic and
188 metamorphic lithic fragments account for roughly equal shares, a dominance of metamorphic
189 fragments is observable. Maturity index values vary between 0.6 and 1.37 (mean MI medial section:
190 1.08; mean MI distal section: 0.89). Among the accessory minerals, micas represent the most abundant
191 constituent (mean share of 2.3% of total rock volume), with minor amounts of heavy minerals.
192 Authigenic minerals are mainly represented by calcite cement which locally also fills the pore spaces
193 derived from partial dissolution of altered plagioclase (Fig. 4F, G).

194 **4.3 Interpretation of the detrital petrology data set**

195 Modal framework compositions of both the San Bartolomeo basal complex and the Bordighera
196 turbidite system suggest a continental block origin (Fig. 5A) according to the classical QtFL tectonic
197 field discrimination plots (cf., Dickinson et al., 1983; Dickinson, 1985). The dominance of
198 monocrystalline quartz over polycrystalline quartz varieties characterizing both units points towards
199 dominantly plutonic parent rocks (e.g., Palomares and Arribas, 1993; Di Giulio et al., 1999; Datta,
200 2005). Minor proportions of polycrystalline quartz characterized by sutured domain boundaries and
201 metamorphic lithic fragments indicate that – albeit to a lesser extent - low-grade metamorphic source
202 rocks contributed to the clastic detritus (Das Gupta and Pickering, 2008). The fact that plagioclase is
203 generally subordinate to alkali feldspar and the low percentages of micas further support the inferred
204 dominant contribution from plutonic source rocks, specifically granitoids (e.g., Palomares and Arribas,

1993; McCann and Arbues, 2012). The QmPK ternary plots (Fig. 5B) reveal no major differences in feldspar varieties´ proportions between the two units. In contrast, the ratios between quartz and feldspar components show a significant up-section shift from the San Bartolomeo Formation to the Bordighera Sandstone (Figs 5A, 6). The San Bartolomeo Fm. samples are characterized by higher quartz proportions and a high degree of sorting, considerably differing from those of the Bordighera Sandstone:

Detrital petrology of the San Bartolomeo Formation samples allows their classification as quartz-rich sandstones to subarkoses (Folk, 1980), with an enhanced textural and compositional maturity (mean maturity index = 2.32; see Fig. 6). This mature character could reflect that these sediments experienced extended transport along continental surfaces characterized by low paleo-relief. The sediments were apparently subjected to prolonged exposure in depositional environments along their pathway from the source area to the final deep-marine sink (e.g., Boggs, 2009; Garzanti et al., 2014). Higher quartz contents in the San Bartolomeo Formation samples moreover imply intense weathering of the less stable grains along relatively low-relief continental land masses (Dickinson and Suczek, 1979).

By contrast, the Bordighera Sandstone samples show balanced proportions of quartz and feldspar and a scarcity of lithic fragments and can thus be classified as ‘‘classic’’ arkosic sandstones (Folk, 1980). Mainly angular to sub-angular grain morphologies and the poor degree of sorting reveal their textural immaturity. The relatively high feldspar content mirrors compositional immaturity (cf., Ghazi and Mountney, 2011). The lower maturity indexes of the Bordighera Sandstone samples (Monte Frontè section: MI = 1.08; Cima di Velega section: MI = 0.89; see Fig. 6), with respect to the underlying San Bartolomeo Fm., indicate shorter transport distances and rapid transportation rates, in a scenario in which sediments were almost directly shed into the deep-marine realm (cf., Zhang et al., 2016). Due to rapid denudation of the source area, no significant reworking that promoted unstable grains to dissolve occurred (e.g., Shanmugam and Moiola, 1988; Mattern, 2005). The observed low degree of both textural and compositional maturity would moreover suggest the dominance of physical weathering processes over chemical weathering (Diekmann and Wopfner, 1996). A first-cycle origin

231 from crystalline source rocks can be inferred, as the greater abundance of chemically and mechanically
232 less stable feldspar grains together with the negligible proportions of sedimentary rock fragments
233 reasonably rule out a recycled provenance from quartz-rich clastic sediments (e.g., Dickinson et al.,
234 1983; Johnsson et al., 1988; Di Giulio et al., 2003; Garzanti et al., 2006).

235 Summarizing, the bulk of the San Bartolomeo Fm. samples fit in the transitional continental-block
236 provenance field, whereas the Bordighera Sandstone samples largely plot in the basement-uplift
237 provenance field. Nonetheless, minor overlapping between the San Bartolomeo Fm. and the
238 Bordighera Sandstone samples is evident in the provenance discrimination field (Fig. 5A) which would
239 imply a somewhat gradual provenance evolution. Notably, the San Bartolomeo Fm. samples
240 accounting for minor overlapping with the Bordighera Sandstone's compositional field were collected
241 from the uppermost part of the formation. Consequently, a fundamentally inverse tectonic stability
242 trend (i.e., from relatively stable to unstable source areas) in between the two units is recorded by
243 detrital petrology (e.g., Dickinson et al., 1983; Garzanti et al., 2014). The possible interpretation of the
244 observed detrital signature evolution is twofold: (1) a different source for clastic sediments forming
245 respectively the San Bartolomeo Fm. and the Bordighera Sandstone, or (2) a common source for both
246 formations that was subjected to a gradual change of regional tectonics resulting in differences in
247 terms of weathering and the depositional setting of the two terrigenous formations. To solve this
248 problem, and at the same time aiming to acquire more precise information about the possible source
249 region for the studied units, U-Pb geochronological study of detrital zircons was undertaken.

250 **5 Results from detrital zircon chronology**

251 **5.1 Age determinations and qualitative comparison of detrital age spectra**

252 LA-ICP-MS age determinations of 108 single grains of the San Bartolomeo Fm. yielded 83 detrital ages
253 (within ±10% of discordance). The analysis of 225 single grains of the Bordighera Sandstone yielded
254 186 concordant ages. Representative cathodoluminescence images are illustrated in Fig. 7, and full
255 isotopic U-Pb analytical data is presented in Supplementary data file 3. Qualitative comparison of the

obtained detrital spectra (normalized probability density plots in Fig. 8) reveals marked similarities in between the analyzed samples. For all the samples, > 85% of the ages younger than 1 Ga fall into the interval between 250 Ma and ca. 650 Ma. All detrital spectra display the most prominent broader peaks of Carboniferous ages around 360 Ma and 300 Ma which account for more than one third of all obtained ages. Additionally, there are significant populations of Silurian and Ordovician ages around 450 Ma and 480 Ma and one distinct Ediacaran peak around 560 Ma. Notably, narrow early- to mid-Permian peaks between ca. 270 Ma and 305 Ma are limited to samples SBF_4, CdV_1 and CdV_3. Significant Cambrian ages have only been determined in samples SBF_4 and CdV_1. Paleo- and Mesoproterozoic ages make up accessory peaks. With respect to their very broad distributions and the fact that these ages do not occur at a comparable magnitude than younger detrital ages, these old populations provide inadequate direct provenance information. The oldest dated grain corresponds to a $^{206}Pb/^{207}Pb$ crystallization age of 3028.5 ±49.9 Ma (SBF_4 sample), whereas the youngest grain reveals a reliable $^{206}Pb/^{238}U$ age of 259.4 ±5.2 Ma (CdV_3 sample).

5.2 Statistical comparison of detrital age spectra

For the purpose of providing a quantitative evaluation of whether the detrital age distributions of the samples from the two formations originated from the same parent rocks, a Kolmogorov-Smirnov test (K-S test) was conducted (e.g., Satkoski et al., 2013; Saylor and Sundell, 2016). In terms of detrital zircon age spectra analysis, the probability calculated (K-S test p-value) represents the probability that two or more randomly selected populations have originated from the same parent population. This degree of dissimilarity between compared age distributions is calculated by the maximum distance in between cumulative probability functions. KS-test p-values >0.05 confirm with a 95% confidence that the compared samples were derived from the same source (e.g., DeGraaff-Surpless et al., 2002; Dickinson and Gehrels, 2009; Satksoski et al., 2013). Cumulative probability functions are shown in Fig. 9A, and the results of the statistical evaluation of age spectra similarities (K-S test p-values) are shown in Fig. 9B. With the single exception of the direct comparison between the MF_1 and CdV_3 samples (p-value of 0.034), all combinations of detrital samples passed the K-S test p-value threshold. Accordingly, based

on the integrated results from modal framework analysis and detrital geochronology, the inference is that the terrigenous successions were derived from the same source terrane.

5.3 Provenance significance of detrital age spectra and relation to potential source areas

With regards to the geochronologically well-defined geodynamic framework of Central and Western Europe (e.g., von Raumer et al., 2003; Linnemann et al., 2004; Dallagiovanna et al., 2009; Handy et al., 2010; Oggiano et al., 2010), the determined detrital zircon age spectra reveal several similarities with age peaks of geochronologically well-defined magmatic and metamorphic events that affected pre-Alpine basement successions. On that premise, the fit between clusters of detrital age populations and regional-scale geodynamic events provides further understanding of the regional paleogeography and the geodynamic setting of the sediment source. The peaks in the detrital zircon age spectra of the San Bartolomeo Fm. and the Bordighera Sandstone directly correspond to geological events recorded in pre-Alpine basement rocks. These age clusters embrace:

- **Ages older than 600 Ma**. This age group comprises Archean ages ranging from ca. 3 Ga to 2.55 Ga that are interpreted to reflect the first event of craton accretion (Cawood et al., 1999). Proterozoic ages spanning an interval from ca. 2000 Ma until 1600 Ma are interpreted as representing the assembly of Laurentia and accretion along its eastern margin (Cawood et al., 1999). Ages related to the assembly of the Rodinia supercontinent, the Greenville orogeny, span an interval from ca. 1200 Ma to 1000 Ma (Li et al., 2008; Meinhold et al., 2013), whereas ages ranging from 1 Ga to ca. 600 Ma can be assigned to the onset of the breakup of Rodinia. Magmatic activity related to preceding rifting occurred from ca. 850 to 750 Ma (e.g., von Raumer et al., 2014).
- **Ages related to the Pan-African / Cadomian orogenic cycles:** This age cluster comprises radiometric ages related to the Cadomian events. These widespread events occurred from ca. 600 Ma to 450 Ma (von Raumer et al., 2014) and represent a series of continental accretions at the margins of Gondwana which were to become involved into the formation of the

supercontinent Pangea. Extensive granitoid emplacement affected the pre-Variscan basement (Linnemann et al., 2008).

- **Ages related to Cambrian rifting stages** date from ca. 530-490 Ma. These crystallization ages are associated with magmatism at the onset of the collapse of the Cadomian orogeny that gave rise to multiple rifting and subduction episodes which marked the evolution of the Rheic ocean (Linnemann et al., 2004; Rossi et al., 2009; Maino et al., 2018). Stampfli et al. (2012) propose the drifting of pre-Variscan blocks away from Gondwana to form the European Hun terranes in the late Cambrian. The assemblage of these continental fragments was accompanied by magmatic pulses along the North African margin.
- **Ages related to Ordovician-Silurian magmatism**. Detrital ages ranging from ca. 490 to 440 Ma are assignable to the continuation of the collapse of the Cadomian orogeny that lead to the opening of the Paleo-Tethys rift and the progressive rifting of the Hun terrane in the Silurian (von Raumer et al., 2003). These early Paleozoic extensional tectonics gave rise to magmatic episodes that are documented to have extensively occurred along the Northern Gondwana margin. Magmatic activity is documented from Sardinia (Oggiano et al., 2010) as well as from the future External massifs (Argentera massif; cf., Rubatto et al., 2001, 2011). Gaggero et al. (2007) reported three distinct phases of magmatism in Sardinia that can be divided into events related to an early Ordovician rifting stage, Middle Ordovician arc volcanism and a late Ordovician to Silurian stage of volcanism resultant from continental drifting.
- **Ages representing events linked to the Variscan orogeny.** Ages spanning from ca. 390 to ca. 320 Ma are interpreted to reflect the continental collision of Gondwana, Laurussia and numerous microcontinental fragments in the Carboniferous. Related magmatic events represent the most widespread zircon age signature among both Tethyan margins (e.g., von Raumer et al., 2003; Beltrán-Triviño et al., 2013) and are represented by a series of granite emplacements (e.g., Calabria: Williams et al., 2012; Fornelli et al., 2016; Sardinia: Pavanetto et al., 2012; Corsica: Giacomini et al., 2006; Casini et al., 2012; Li et al., 2014; Ligurian Alps:

Dallagiovanna et al., 2009; Maino et al., 2012; Internal Western Alps massifs: Dora Maira: Sandrone et al., 1993; Manzotti et al., 2016; External massifs: Mont Blanc, Argentera: Ménot et al., 1994; Rubatto et al., 2001, 2011). Importantly, Variscan magmatic episodes are preferably recorded in the paleo-European basement in comparison to that of the Southern Alps (Linnemann et al., 2008; cf., Beltrán-Triviño et al., 2013).

- **Ages associated with post-Variscan magmatism** (ca. 300-280 Ma) are attributable to gravitational collapse of the thickened Variscan orogenic crust (McCann et al., 2006). Alternating transpressional and transtensional tectonic regimes promoted the development of continental basins in Central and Western Europe. Characteristic graben and half-graben structures are typically associated with syntectonic volcanic activity. Magmatic activity related to the initial orogen collapse is mostly documented from Calabria (Liotta et al., 2008), Sardinia (Ronca et al., 1999; Gaggero et al., 2017), and Corsica (Cabanis et al., 1990) as well as from the Southern Alps (e.g., Quick et al., 2009; Berra et al., 2014).
- **Ages attributed to mid-Permian to Lower Triassic magmatism** range from ca. 270 Ma to 240 Ma. Recent research documents a later stage of volcanism restricted to the Southern Alps (Beltrán-Triviño et al., 2013), Calabria (Fornelli et al., 2011), Sardinia and Corsica (Traversa et al., 2003; Gaggero et al., 2007), as well as to the Ligurian Alps (Dallagiovanna et al., 2009; Maino et al., 2012). These latter events are related to intense magmatic activity interpreted to reflect the onset of drifting since the Middle Triassic and might therewith epitomize the beginning of the Alpine cycle (cf., Beltrán-Triviño et al., 2013). It should be noted that these later-stage volcanic episodes can be separated from the post-Variscan magmatic events by a period of strike-slip activity and intermittent granite emplacement (cf., McCann et al., 2006).

6 Source area inference

Detrital modal assemblages of both the basal complex (San Bartolomeo Formation) and the coarse-clastic turbidite system (Bordighera Sandstone) indicate that predominantly upper crustal rocks – mainly granitoid plutons - provided the source rocks. Minor contributions by low-grade metamorphic

359 rocks are recorded by very minor proportions of metamorphic lithic fragments. Owing to dissimilar
360 architectures of the bounding margins of the Piedmont-Ligurian ocean, different levels of the
361 continental crust were exposed (e.g., Müntener and Hermann, 2001; Bracciali et al., 2007; Malusà et
362 al., 2015; Decarlis et al., 2017). According to Froitzheim and Manatschal (1996), the opening of the
363 Piedmont-Ligurian ocean occurred in two stages. The initial rifting stage, assigned to the late Triassic
364 to early Jurassic, was typified by the development of listric fault systems which represent symmetric
365 lithosperic stretching. Contrastingly, in the early-middle Jurassic, lithosperic-scale detachment faults
366 developed that facilitated passive asymmetric extension. The paleo-European margin comprised a
367 crustal section mostly composed of granitoids and low-grade metamorphic rocks, whereas the Adriatic
368 margin exposed a full crustal lithospheric section that also included high-grade metamorphic rocks (cf.,
369 Bracciali et al., 2007).

370 The sandstone detrital modes of the two successions reveal the dominance of plutonic constituents
371 and for that reason suggest a paleo-European provenance. The integration of the results from detrital
372 zircon chronology confirms the presumption that the paleo-European (i.e., the Northern Tethyan)
373 margin provided the bulk of the clastic detritus. Essentially the dominant peaks related to the onset of
374 the Variscan cycle that typify the detrital spectra allow to rule out a source terrane located in the
375 Adriatic margin (cf., Bütler et al., 2011; Beltrán-Triviño et al., 2013). In particular, the distinct peaks of
376 Mississippian ages (ca. 330 to 355 Ma) are absent in crystalline suites of the Adriatic margin (i.e., in the
377 Sesia microfragment; e.g., Klötzli et al., 2014; Malusà et al., 2015). Moreover, the occurrence of
378 Cambrian detrital zircons provides further evidence for a source terrane located in the European
379 margin (Rossi et al., 2009; see also Thomas et al., 2010 and Fornelli et al., 2015 for discussions on
380 European and ‘‘African’’ provenance signatures).

381 In combination with the prominent Carboniferous to lower Permian detrital age peaks, the data
382 discussed above suggests that dominantly plutonic source terranes distributed along the margins of
383 the composite crystalline Southern Variscan belt margins represent potential source areas. According
384 to paleogeographic maps (e.g., von Raumer et al., 2002; Casini et al., 2015), the Variscan and pre-

385 Variscan continental basement assemblages of the Briançonnais, the Dora-Maira Massif (as part of the
386 internal massifs of the proximal European margin), the Argentera Massif of the External Massifs, as
387 well as the Corsica-Sardinia Batholith and the Calabrian granitoid massifs need to be taken into
388 consideration. Although no paleocurrent indicators for the San Bartolomeo Fm. could be identified,
389 analysis of paleocurrent indicators for the Bordighera Sandstones reveals a reasonably unidirectional
390 (present-day) N-NE orientation of the main sediment flux. This is also confirmed by the distinct South-
391 North directed facies trend characterizing the Bordighera Sandstone (see paleocurrent rose in Fig. 2A
392 and Mueller et al., 2017, for details on facies distribution). Therefore, the source terrane must have
393 been located in the SSW of the Bordighera turbidite system and candidate source areas can thus be
394 narrowed to the Corsica-Sardinia block and the Calabrian massifs. Both terranes record
395 geochronologically well-constrained evidence of magmatic and metamorphic pulses which are readily
396 compatible with peaks of the detrital spectra (e.g., Giacomini et al., 2006, 2007; Gaggero et al., 2007,
397 2017; Liotta et al., 2008; Rossi et al., 2009; Oggiano et al., 2010; Casini et al., 2012; Pavanetto et al.,
398 2012; Williams et al., 2012; Langone et al., 2014; Li et al., 2014; Fornelli et al, 2016). However, taking
399 the abundant late Neoproterozoic ages of the detrital spectra into account, the Calabrian massifs can
400 be ruled out, since the occurrence of late Ediacaran (pronounced peak around 650 Ma) magmatic
401 activity or metamorphic phases have not been documented from Calabria (cf., Liotta et al., 2008;
402 Williams et al., 2012; Fornelli et al., 2016). In particular, the marked similarity between Devonian to
403 early Permian detrital zircon age peaks of the investigated sediments (see synthetic probability density
404 plots of all obtained detrital ages in Fig 10) and pulses of crystallization ages that define the Sardo-
405 Corsican batholiths (i.e., ca. 345-337 Ma "Durbachites" from NW Corsica of Paquette et al., 2003, and
406 the ca. 325-285 Ma U2 and U3 suites of Casini et al., 2012, 2015) suggest that the Corsica-Sardinia
407 block is the primary source area for both terrigenous formations of the San Remo-Monte Saccarello
408 Unit. Such a scenario has previously been proposed solely based on paleocurrent analysis and
409 observations on grain composition (e.g., Vanossi, 1965; Sestini, 1970; Sagri, 1980, 1984) and is
410 herewith confirmed by means of coupling petrographic analysis with U-Pb detrital zircon chronology.

411

412 **7. Discussion**

413 **7.1 Comparison to proposed provenance models for flysch successions of the Piemont-Ligurian**
414 **ocean**

415 Numerous provenance studies addressed pre-collisional flysch successions of the Northern Apennines
416 (e.g., Sagri and Marri, 1980; Valloni and Zuffa, 1984; Wildi, 1985, 1987; Rowan, 1990; Fontana et al.,
417 1994; van de Kamp and Leake, 1995; Argnani et al., 2006; Bracciali et al., 2007). Flysch sedimentation
418 occurred in two distinct paleogeographic domains, the Internal and the External Ligurian Units
419 (Marroni et al., 2001). The Internal Ligurian Units represent a continuous succession ranging from the
420 Jurassic ophiolites through Cretaceous and Paleocene turbidite successions, whereas in the External
421 Ligurian Units the sedimentary succession became detached from their underlying oceanic crust
422 substrate. Siliciclastic successions of the Internal Ligurian Units have generally been attributed to a
423 European provenance (e.g., Fontana et al., 1994; Bracciali et al., 2007). By contrast, the External
424 Ligurian Units have been interpreted as representing the distal Adriatic margin and the transition
425 towards the Piemont-Ligurian ocean and are hence associated to an Adriatic provenance. Among the
426 Upper Cretaceous to Paleocene Internal Ligurian successions, Valloni and Zuffa (1984) report quartzo-
427 feldspathic arkoses from the ‘‘Arenarie Superiori’’ (i.e., the Gottero Sandstone) and the Monghidoro
428 Formation which are defined by similar primary modal parameters to the ones documented in the
429 present study (Gottero Sandstones: mean Qt51F39L10; Monghidoro Formation: mean Qt59F38L3).
430 Supplementary petrographic studies by Van de Kamp and Leake (1995) and Pandolfi (1996)
431 documented similar compositions (mean Qt42F55L3 and Qt50F33L17, respectively) for the Gottero
432 Sandstone. These compositions are reasonably similar to the results derived from the Bordighera
433 Sandstones (mean Qt49F48L3). Wildi (1985) defined a zircon-tourmaline-rutile dominated heavy
434 mineral association as being characteristic for the Paleo-European margin and consequently claimed
435 the European margin source for the Upper Cretaceous Flysch Units deposited in the Piemont-Ligurian

ocean. Wildi (1987) also questioned the ‘‘passive’’ margin configuration of the European Tethyan margin and proposed a late Cretaceous inversion of the European margin that provided a Corsica-derived source for siliciclastic successions intercalated into Helminthoid Flysch sequences, among which the San Remo-Monte Saccarello Unit (i.e., the Bordighera Sandstone) was positioned.

Available datasets from recent studies on detrital zircon assemblages of Upper Penninic flysch successions (Chu et al., 2016; Lin et al., 2018) allow a comparison of the detrital suites of this study. No overlap can be identified with allochthonous successions of Internal Liguride affinity (e.g., Pandolfi et al., 2016; Marroni et al., 2017) which were incorporated into both the Piedmont Nappe and the Balagne Nappe (Fig. 11). In contrast, the qualitative comparison reveals a striking similarity with the Eocene Annunciata Fm. that is now overthrust onto Corsica (cf., Lin et al., 2018). Notably, the Annunciata Fm., although treated as allochthonous (Egal, 1992), has more recently been considered as having undergone minor displacement and being positioned in proximity to its original depositional location (cf. Marroni et al., 2001; Lin et al., 2018). In addition, the detrital chronology signature of the pre-collisional Upper Cretaceous Schistes Lustrès presented by Chu et al. (2016) displays strong similarities as the major detrital age population peaks around 330 Ma. Either way, based on the presence of Proterozoic age peaks, Chu et al. (2016) do not clearly assign the Schistes Lustrès to either a European or an Adriatic provenance, as these old detrital ages might reflect a complex inheritance of the detrital zircon grains or the detrital zircons could be polycyclic.

7.2 Control mechanism for re-activation of the paleo-European margin

The documentation of major sand supply from a source area located along the lower European plate requires an explanation. Evidence for emersion of the Sardo-Corsican block is provided by the presence of Albian bauxite deposits superimposing Oxfordian to Aptian shallow to transitional marine carbonates that imply subaerial exposure (Mameli et al., 2007). Mameli et al. (2007) follow the interpretation of a transpressive tectonic regime development suggested by Puigdefabregas and Souquet (1986) as the key control on continental block uplift. However, according to the observations

presented in this study, the stratigraphic evolution linked to sediment maturity implies that the reactivation of the margin of the lower European plate occurred in a craton-ward prograding orientation.

According to our interpretation, the development of a flexural forebulge due to lithospheric flexure caused by the tectonic loading of the overthrust wedge is considered as better explaining the key tectonic control on re-activating the hyper-extended paleo-European margin (e.g., Stockmal et al., 1987; Barbieri et al., 2004). The craton-ward migration of its hinge line (e.g., DeCelles and Giles, 1996; Einsele, 2000) is mirrored by a gradual provenance evolution from the highly mature sediments of the San Bartolomeo Formation towards the highly immature Bordighera Sandstone (see conceptual models in Fig. 12) within a framework similar to the one proposed by Stockmal et al. (1987) for a passive continental margin arriving in a subduction zone.

Specifically, during the Hauterivian to Santonian, the craton-ward passing hinge line of the flexural bulge affected the distal European margin, and this is interpreted to have resulted in the tectonic instability along the shelfal areas of the passive margin, where terrigenous sediments were subjected to reworking processes before being re-sedimented into the trench. Such reworking can explain the textural maturity of the sediments of the San Bartolomeo Fm. Afterwards, during the Campanian to Maastrichtian, the NNW-prograding hinge line of the flexural bulge arrived in the hinterland part of the margin and triggered the uplift of crustal blocks promoting rapid sedimentation of the first-cycle coarse-clastic detritus of the Bordighera Sandstone into the trench.

The migration of the flexural bulge parallel to the Frontal Penninic Thrust can straightforwardly be integrated into paleogeographic and tectonic models that address the reconstruction of the evolution of the Western Alps. These models demonstrate that deformation and metamorphism stepwise migrated in a NW-ward directed orientation (e.g., Schmid et al. 1996; Lister et al., 2001; Rosenbaum and Lister 2005; Handy et al. 2010). However, it should be noted that the spatial and temporal magnitudes of the deformation remain poorly constrained (Lister et al., 2001; Ford et al., 2006). Based

on tectonostratigraphic relationships of sedimentary cover successions of the Briançonnais domain, a flexural forebulge development has previously been proposed (Michard and Martinotti, 2002). Michard and Martinotti (2002) suggest that late Cretaceous to Eocene disconformities mirror the passage of a flexural bulge through the distal European margin and propose a bulge amplitude of ca. 800-1000 m which resulted in extensional faulting of the uplifted continental blocks and an enhanced sediment supply. Such a scenario can readily explain the reciprocal trend in sediment maturity from passive margin-fed quartz-rich sandstones of the basal complex towards the immature Bordighera Sandstone arkoses that is documented in this study.

8. Conclusions

The multi-proxy sediment provenance study of the two terrigenous members of the pre-collisional San Remo-Monte Saccarello Unit of the Western Ligurian Flysch complex gains a better understanding of the pre-collisional evolution of the Piedmont-Ligurian ocean and its bounding continental margins. The main conclusions are summarized as follows:

- Petrographic analyses of the terrigenous sediments reveal an upsection transition from mature, fine-grained, quartz-rich basin plain turbidite sandstones (San Bartolomeo Formation) towards first-cycle coarse-grained arkoses (Bordighera Sandstone). The onset of coarse-clastic sedimentation is interpreted to mark a substantial modification of the geodynamic regime. Increased sediment yield and sediment caliber result from the increased slope gradient caused by rapid basement uplift (Dickinson et al., 1983). Albeit the comparison of the textural character of the two members documents a marked difference in terms of sediment maturity, average modal framework compositions suggest a more gradual provenance evolution which is interpreted to mirror the exhumation of a crystalline basement terrane during the pre-collisional stage of the Alpine convergence.
- Geochronological data (U-Pb detrital zircon ages) provide evidence that, despite the observed compositional change, the terrigenous successions were derived from the same source

terrane. In combination with results from detrital petrography, these observations document that the source area underwent significant tectonic modification from a relatively stable craton to a basement uplift setting.

- Peaks in the detrital age spectra fit with well-documented magmatic and metamorphic pulses that affected the pre-Alpine basements and allow for the identification of the lower plate passive European continental margin as the primary source of the clastic detritus. More specifically, integrating geochronological ages with paleocurrent indicators shows that the proposed provenance from the Corsica-Sardinian block is confirmed.
- In the context of the Alpine subduction, this evidence argues for tectonic activity along the passive continental margin of the subducted plate that provided the major sand supply area for the clastic sediment delivered into the subduction zone.

The craton-ward migration of the flexural bulge developed in response to the tectonic loading of the advancing Alpine accretionary wedge and explains the re-activation and tectonic inversion of the passive paleo-European margin. This implies that the detrital evolution documented in this work reflects the activation of the passive continental margin arriving in the subduction zone.

In a broad geodynamic context, based on the present study, we suggest that the tectonic inversion of a passive continental margin arriving in a subduction zone results in a recognizable petrographic signature in the detrital record of deep-sea sequences. Therefore, this signature provides a potential though often overlooked record of the imminent transition from subduction to collision of ancient collisional systems.

Acknowledgements

Financial support was provided by the University of Pavia PhD research grant for Pierre Mueller. Fieldwork and laboratory expenses were supported by generous contributions from the Turbidites Research Group (TRG) sponsors (AkerBP, BP, ConocoPhilips, Equinor, ENI, Hess, Murphy Oil

538 Corporation, OMV and Shell). We are indebted to Gaia Militello and Laura Gaggero (University of
539 Genova), as well as Michela Idiomi and Andrea Ortenzi (ENI S.p.A. San Donato Milanese) for assistance
540 with zircon cathodoluminescence imaging. Matteo Maino and Massimiliano Zattin are thanked for
541 providing valuable comments on earlier versions of the draft. We are grateful to journal editor Jasper
542 Knight, Luca Barale and an anonymous reviewer who provided constructive suggestions and helpful
543 comments.

544

545 Appendix

546 Appendix A: Full modal framework data

547 Appendix B: Methodology and analytical setup of detrital zircon chronology analysis

548 Appendix C: Full detrital zircon isotopic data

549 Appendix D: Zircon standard tables

550

551 **References**

552 Alvarez, W., Shimabukuro, D.H., 2009. The geological relationships between Sardinia and Calabria
553 during Alpine and Hercynian times. Italian Journal of Geosciences 128, 257-268.

554 Andersen, T., 2005. Detrital zircons as tracers of sedimentary provenance: limiting conditions from
555 statistics and numerical simulations. Chemical Geology 40, 249-270.

556 Argnani, A., Fontana, D., Stefani, C., Zuffa, G.G., 2006. Palaeogeography of the Upper Cretaceous-
557 Eocene carbonate turbidites of the northern Apennines from provenance studies. In: Moratti, G.,
558 Chalouan, A. (Eds.), Tectonics of the western Mediterranean and North Africa. Geological Society
559 of London, Special Publications 262, pp. 259-275.

560 Barbieri, C., Bertotti, G., Di Giulio, A., Fantoni, R., Zoetemeijer, R., 2004. Flexural response of the
561 Venetian foreland to the Southalpine tectonics along the TRANSALP profile. Terra Nova 16, 273-
562 280.

563 Beltrán-Triviño, A., Winkler, W., von Quadt, A., 2013. Tracing Alpine sediment sources through laser
564 ablation U–Pb dating and Hf-isotopes of detrital zircons. Sedimentology 60, 197-224.

565 Berra, F., Tiepolo, M., Caironi, V., Siletto, G.B., 2014, U–Pb zircon geochronology of volcanic deposits
566 from the Permian basin of the Orobic Alps (Southern Alps, Lombardy): chronostratigraphic and
567 geological implications. Geological Magazine, 152, 429-443.

568 Bhatia, M.R., 1983. Plate tectonics and geochemical composition of sandstones. The Journal of Geology
569 91, 611–627.

570 Boggs, S., 2009, Petrology of Sedimentary Rocks (2nd edition). Cambridge University Press, Cambridge
571 CB2 8RU, UK.

572 Bousquet R., Oberhänsli R., Goffé B., Wiederkehr M., Koller F., Schmid S.M., Schuster R., Engi M.,
573 Berger A.,Martinotti G., 2008. Metamorphism of metasediments in the scale of an orogen: A key
574 to the Tertiary geodynamic evolution of the Alps. In: Siegesmund, S., Fügenschuh, B., Froitzheim,
575 N. (Eds.), Tectonic Aspects of the Alpine-Dinaride-Carpathian System, Geological Society of
576 London, Special Publications 298, pp. 393-412.

577 Bracciali L., Marroni M., Pandolfi L., Rocchi S, 2007. Geochemistry and petrography of Western Tethys
578 Cretaceous sedimentary covers (Corsica and Northern Apennines): from source area to
579 configuration of margins. In: Arribas J., Critelli S., Johnsson M.J. (Eds.), Sedimentary Provenance
580 and Petrogenesis: Perspectives From Petrography and Geochemistry, Geological Society of
581 America, Special Paper 420, pp. 73-93.

582 Bracciali, L., Najman, Y., Parrish, R.R., Akhter, S.H., Millar, I., 2014. The Brahmaputra tale of tectonics
583 and erosion: Early Miocene river capture in the Eastern Himalaya. Earth and Planetary Science
584 Letters 415, 25-37.

585 Bütler, E., Winkler, W., Guillong, M., 2011. Laser ablation U/Pb age patterns of detrital zircons in the
586 Schlieren Flysch (Central Switzerland): new evidence on the detrital sources. Swiss Journal of
587 Geosciences 104, 225-236.

588 Cabanis, B., Cocheme, J.J., Vellutini, P.J, Joron, J.L., Treuil, M., 1990. Post-collisional Permian volcanism
589 in northwestern Corsica: an assessment based on mineralogy and trace-element geochemistry.
590 Journal of Volcanology and Geothermal Research 44, 51-67.

591 Caron, C., Hesse, R., Kerckhove, C., Homewood, P., Van Stuijvenberg, J., Tasse, N., Winkler, W., 1981.
592 Comparaison préliminaire des flyschs a Helminthoïdes sur troi transverales des Alpes. Eclogae
593 Geologicae Helvetiae 74, 369-378.

594 Casini, L., Cuccuru, S., Maino, M., Oggiano, G., Tiepolo, M., 2012. Emplacement of the Arzachena Pluton
595 (Corsica–Sardinia Batholith) and the geodynamics of incoming Pangaea. Tectonophysics 544-545,
596 31-49.

597 Casini, L., Cuccuru, S., Puccini, A., Oggiano, G., Rossi, P., 2015. Evolution of the Corsica–Sardinia
598 Batholith and late-orogenic shearing of the Variscides. Tectonophysics 646, 65–78.

599 Cawood, P.A., Nemchin, A.A., Leverenz, A., Saeed, A., Ballance, P.F., 1999. U/Pb dating of detrital
600 zircons: Implications for the provenance record of Gondwana margin terranes. Geological Society
601 of America Bulletin 111, 1107-1119.

602 Chu, Y., Lin, W., Faure, M., Wang, Q., 2016. Detrital zircon U-Pb ages and Hf isotopic constraints on the
603 terrigenous sediments of the Western Alps and their paleogeographic implications. Tectonics 35,
604 1-20.

605 Cobianchi, M., Di Giulio, A., Galbiati, B., Mosna, S., 1991. Il ‘‘complesso di base’’ del Flysch di S. Remo
606 nell’area di S. Bartolomeo, Liguria occidentale (nota preliminare). Atti Ticinesi Scienze della Terra
607 34, 145–154.

608 Dallagiovanna, G., Gaggero, L., Maino, M., Seno, S., Tiepolo, M., 2009. U–Pb zircon ages for post-
609 Variscan volcanism in the Ligurian Alps (northern Italy). Journal of the Geological Society 166,
610 101–114.

611 Dal Piaz, G.V., Bistacchi, A., Massironi, M., 2003. Geological outline of the Alps. Episodes 26, 175-180.

612 Das Gupta, K., Pickering, K.T., 2008. Petrography and temporal changes in petrofacies of deep-marine
613 Ainsa-Jaca basin sandstone systems, Early and Middle Eocene, Spanish Pyrenees. Sedimentology
614 55, 1083-1114.

615 Datta, B., 2005. Provenance, tectonics and palaeoclimate of Proterozoic Chandarpur sandstones,
616 Chattisgarh Basin: a petrographic view. Journal of Earth Sciences 114, 227-245.

617 Decarlis, A., Dallagiovanna, G., Lualdi, M., Maino, M., Seno, S., 2013. Stratigraphic evolution in the
618 Ligurian Alps between Variscan heritages and the Alpine Tethys opening: a review. Earth- Science
619 Reviews 125, 43-68.

620 Decarlis, A., Fellin, M.G., Maino, M., Ferrando, S., Manatschal, G., Gaggero, L., Seno, S., Stuart, F.M.,
621 Beltrando, M., 2017. Tectono-thermal Evolution of a Distal Rifted Margin: Constraints from the
622 Calizzano Massif (Prepiedmont-Briançonnais Domain, Ligurian Alps). Tectonics 36, 3209-3228.

623 DeCelles, P.G., Giles, K.A., 1996. Foreland basin systems. Basin Research 8, 105-123.

624 DeGraff-Surpless, K., Graham, S.A., Wooden., J.L., McWilliams, M.O., 2002. Detrital zircon provenance
625 analysis of the Great Valley Group, California: Evolution of an arc-forearc system. Geologic Society
626 of America Bulletin 114, 1564-1580.

627 Dickinson, W.R., 1985, Interpreting Provenance Relations from Detrital Modes of Sandstones. In: Zuffa,
628 G.C., Ed., Provenance of Arenites, D. Reidel Publishing Company, Dordrecht, The Netherlands,
629 333-362.

630 Dickinson, W.R., Beard, L.S., Brakenridge, G.R., Erjavec, J.L., Ferguson, R.C., Inman, K.F., Knepp, R.A.,
631 Lindberg, F.A., Ryberg, P.T., 1983. Provenance of North American Phanerozoic sandstones in
632 relation to tectonic setting. Geological Society of America Bulletin 94, 222–235.

633 Dickinson, W.R., Gehrels, G.E., 2009. Use of U-Pb ages of detrital zircons to infer maximum depositional
634 ages of strata: A test against a Colorado Plateau Mesozoic database. Earth and Planetary Science
635 Letters 288, 115-125.

636 Dickinson, W.R., Suczek, C., 1979. Plate tectonics and sandstone compositions. American Association
637 of Petroleum Geologists Bulletin 63, 2164–2182.

638 Diekmann, B., Wopfner, H., 1996. Petrographic and diagenetic signatures of climatic change in periand
639 postglacial Karoo Sediments of SW Tanzania. Palaeogeography, Palaeoclimatology, Palaeoecology
640 125, 5-25.

641 Di Giulio, A., 1992. The evolution of the Western Ligurian Flysch Units and the role of mud diapirism in
642 ancient accretionary prisms (Maritime Alps, Northwestern Italy). International Journal of Earth
643 Sciences (Geologische Rundschau) 81, 655-668.

644 Di Giulio, A., Ceriani, A., Ghia, E., Zucca, F., 2003, Composition of modern stream sands derived from
645 sedimentary source rocks in a temperate climate (Northern Apennines, Italy). Sedimentary
646 Geology 158, 145-161.

647 Di Giulio A., Galbiati B., 1985. Quarzareniti nel complesso di base del Flysch di San Remo (Alpi
648 Marittime). Bollettino della Società Geologica Italiana 8, 65-68.

649 Di Giulio, A, Galbiati B., 1991. Le facies caotiche della Liguria occidentale: un nuovo modello
650 interpretativo. Atti Ticinesi Scienze della Terra 34, 155-160.

651 Di Giulio, A., Ronchi, A., Sanfilippo, A., Balgord, E.A., Carrapa, A., Ramos, V.A., 2017, Cretaceous
652 evolution of the Andean margin between 36°S and 40°S latitude through a multi-proxy
653 provenance analysis of Neuquen Basin strata (Argentina). Basin Research, 29, 284-304.

654 Di Giulio, A., Tribuzio, R., Ceriani, A., Riccardi, M.P., 1999, Integrated analyses constraining the
655 provenance of sandstones, a case study: The Section Peak Formation (Beacon Supergroup,
656 Antarctica). Sedimentary Geology 124, 169-183.

657 Di Giulio, A., Valloni, R., 1992, Analisi microscopia delle arentiti terrigene: Parametri petrologici e
658 composizioni modali. Acta Naturalia de l´Ateneo Parmese 28, 55-101.

659 Dunkl, I., Di Giulio, A., Kuhlemann, J., 2001. Combination of single-grain fission track chronology and
660 morphological analysis of detrital zircon crystals in provenance studies—sources of the Macigno
661 formation (Apennines, Italy). Journal of Sedimentary Research 71, 516–525.

662 Egal, E., 1992. Structures and tectonic evolution of the external zone of Alpine Corsica. Journal of
663 Structural Geology 14, 1215-1228.

664 Einsele, G., 2000. Sedimentary Basins: Evolution, Facies and Sediment Budget (2nd edition). Springer
665 Verlag, Berlin, Heidelberg.

666 Fedo, C.M., Sircombe, K.N., Rainbird, R.H., 2003. Detrital zircon analysis of the sedimentary record.
667 Reviews in Mineralogy and Geochemistry 53, 277-303.

668 Folk, R.L., 1980. Petrology of Sedimentary Rocks (second edition). Hemphill's Publishing Co., Austin,
669 TX.

670 Fontana, D., Spadafora, E., Stefani, C., Stocchi, S., Tateo, F., Villa, G., Zuffa, G.G., 1994. The Upper
671 Cretaceous Helminthoid Flysch of the Northern Apennines: Provenance and Sedimentation.
672 Memorie della Società Geologica Italiana 48, 237-250.

673 Ford, M., Duchene, S., Gasquet, D., Vanderhaeghe, O., 2006. Two-phase orogenic convergence in the
674 external and internal SW Alps. Journal of the Geological Society 163, 815–826.

675 Fornelli, A., Langone, A., Micheletti, F., Piccareta, G., 2011. Time and duration of Variscan high
676 temperature metamorphic processes in the south European Variscides: constraints from U-Pb
677 chronology and trace element chemistry of zircon. Mineralogy and Petrology 103, 101–122.

678 Fornelli, A., Micheletti, F., Langone, A., Perrone, V., 2015. First U–Pb detrital zircon ages from Numidian
679 sandstones in Southern Apennines (Italy): Evidences of African provenance. Sedimentary Geology
680 320, 19-29.

681 Fornelli A., Micheletti F., Piccarreta, G., 2016. Late-Proterozoic to Paleozoic history of the peri-
682 Gondwana Calabria–Peloritani Terrane inferred from a review of zircon chronology. Springerplus
683 5, 1-19, doi: 10.1186/s40064-016-1839-8.

684 Froitzheim, N., Manatschal, G., 1996. Kinematics of Jurassic rifting, mantle exhumation, and passive
685 margin formation in the Austroalpine and Penninic nappes (eastern Switzerland). Bulletin of the
686 Geological Society of America 108, 1120–1133.

687 Froitzheim, N., Plašienka, D., Schuster, R., 2008. Alpine tectonics of the Alps and Western Carpathians.
688 In: McCann, T. (ed.), The Geology of Central Europe. Volume 2: Mesozoic and Cenozoic, Geological
689 Society Publishing House, London, pp. 1141-1232.

690 Gaggero, L., Gretter, N., Langone, A., Ronchi, A., 2017. U-Pb geochronology and geochemistry of late
691 Palaeozoic volcanism in Sardinia (southern Variscides). Geoscience Frontiers 8, 1263-1284, doi:
692 10.1016/j.gsf.2016.11.015.

693 Gaggero, L., Oggiano, G., Buzzi, L., Slejko, F., Cortesogno, L., 2007. Post-Variscan mafic dikes from the
694 late orogenic collapse to the Tethyan rift: evidences from Sardinia. Ofioliti 32, 15–37.

695 Galbiati, B., Cobianchi, M., 1997. L'indipendenza tettonica dell'unita di Sanremo rispetto all'unita di
696 Moglio-Testico. Bolletino della Società Geologica Italiana 116, 453–472.

697 Garzanti, E., Andò, S., Vezzoli, G., 2006. The Continental Crust as a Source of Sand (Southern Alps Cross
698 Section, Northern Italy). The Journal of Geology 114, 533-554.

699 Garzanti, E., Doglioni, C., Vezzoli, G. Andò, S., 2007. Orogenic belts and orogenic sediment provenance.
700 The Journal of Geology 115, 315–334.

701 Garzanti, E., Vermeesch, P., Padoan, M., Resentini, A., Vezzoli, G., Ando, S., 2014. Provenance of
702 Passive-Margin Sand (Southern Africa). The Journal of Geology 122, 17-42.

703 Gasinski, A., Slaczka, A., Winkler, W., 1997. Tectono-sedimentary evolution of the Upper Prealpine
704 nappe (Switzerland and France): nappe formation by Late Cretaceous-Paleogene accretion.
705 Geodinamica Acta 10, 137-157.

706 Gehrels, G.E., Valencia, V.A., Joaquin, R., 2009, Enhanced precision, accuracy, and efficiency, and
707 spatial resolution of U-Pb ages by laser ablation-multicollector-inductively coupled plasma mass
708 spectrometry. Geochemistry Geophysics Geosystems. 9, 1-13.

709 Ghazi, S., Mountney, N.P., 2011. Petrography and provenance of the Early Permian Fluvial Warchha
710 Sandstone, Salt Range, Pakistan. Sedimentary Geology 233, 88-110.

711 Giacomini, F., Bomparola, R.M., Ghezzo, C., Guldbransen, H., 2006. The geodynamic evolution of the
712 Southern European Variscides: constraints from the U/Pb geochronology and geochemistry of the
713 lower Palaeozoic magmatic-sedimentary sequences of Sardinia (Italy). Contributions to
714 Mineralogy and Petrology 152, 19–42.

715 Giacomini, F., Braga, R., Tiepolo, M., Tribuzio, R., 2007. New constraints on the origin and age of
716 Variscan eclogitic rocks (Ligurian Alps, Italy). Contributions to Mineralogy and Petrology 153, 29–
717 53.

718 Giammarino, S., Fanucci, F., Orezzi, S., Rosti, D., Morelli, D., 2010. Foglio 258–271 San Remo. Note
719 illustrative della carta geologica d'Italia alla scala 1:50.000. Roma: Servizio Geologico d'Italia.

720 Handy, M.R., Schmid, S.M., Bousquet, R., Kissling, E., Bernoulli, D., 2010. Reconciling plate-tectonic
721 reconstructions with the geological–geophysical record of spreading and subduction in the Alps.
722 Earth-Science Reviews 102, 121-158.

723 Handy, M.R., Ustaszewski, K., Kissling, E., 2014. Reconstructing the Alps–Carpathians–Dinarides as a
724 key to understanding switches in subduction polarity, slab gaps and surface motion. International
725 Journal of Earth Sciences (Geologische Rundschau) 104, 1-26.

726 Ingersoll, R.V., Bullard, T.F., Ford, R.D., Grimm, J.P., Pickle, J.D., Sares, S.W., 1984. The effect of grain
727 size on detrital modes: a test of the Gazzi-Dickinson point-counting method. Journal of
728 Sedimentary Petrology 54, 103–116.

729 Johnsson, M.J., Stallard, R.F., Meade, R.H., 1988. First-cycle quartz arenites in the Orinoco River basin,
730 Venezuela and Colombia. Journal of Geology 96, 263-277.

731 Klötzli, U. S., Sinigoi, S., Quick, J.E., Demarchi, G., Tassinari, C.C.G., Sato, K., Günes, Z., 2014. Duration
732 of igneous activity in the Sesia Magmatic System and implications for high-temperature
733 metamorphism in the Ivrea–Verbano deep crust. Lithos 206–207, 19–33.

734 Langone, A., Caggiannelli, A., Festa, V., Prosser, G., 2014. Time Constraints on the Building of the Serre
735 Batholith: Consequences for the Thermal Evolution of the Hercynian Continental Crust Exposed
736 in Calabria (Southern Italy). The Journal of Geology 122, 183-199.

737 Lanteaume, M., 1962. Considérations paléogéographiques sur la patrie supposée des nappes de flysch
738 a Helminthoides des Alpes et des Apennins, Bulletin de la Société géologique de France 7, 627–
739 643.

740 Lanteaume, M., Radulescu, N., Gavos, M., Feraud, J., 1990. Notice Explicative, Carte Geol. De France
741 (1 : 50.000), Feuille Vieve-Tende (948). BRGM, Orleans, 139 pp.

742 Li, Z.X., Bogdanova, S.V., Collins, A.S., Davidson, A., 2008. Assembly, Configuration, and Break-up
743 History of Rodinia: A Synthesis. Precambrian Research 160, 179–210.

744 Li, X.H., Faure, M., Lin, W., 2014. From crustal anatexis to mantle melting in the Variscan orogen of
745 Corsica (France): SIMS U–Pb zircon age constraints. Tectonophysics 634, 19–30.

746 Lin, W., Rossi, P., Faure, M., Li, X.-H., Ji, W., Chu, Y., 2018. Detrital zircon age patterns from turbidites
747 of the Balagne and Piedmont nappes of Alpine Corsica (France): Evidence for an European margin
748 source. Tectonophysics 722, 69-105.

749 Linnemann, U., McNaughton, N., Romer, R.L., Gehmlich, M., Drost, K., Tonk, C., 2004. West African
750 provenance for Saxo-Thuringia (Bohemian Massif): Did Armorica ever leave pre-Pangean
751 Gondwana? – U/Pb-SHRIMP zircon evidence and the Nd-isotopic record. International Journal of
752 Earth Sciences (Geologische Rundschau) 93, 683–705.

753 Linnemann, U., Pereira, F., Jeffries, T.E., Drost, K. and Gerdes, A., 2008. The Cadomian Orogeny and
754 the opening of the Rheic Ocean: The diachrony of geotectonic processes constrained by LA-ICP-
755 MS U–Pb zircon dating (Ossa-Morena and Saxo-Thuringian Zones, Iberian and Bohemian Massifs).
756 Tectonophysics 461, 21–43.

757 Liotta, D., Caggianelli, A., Kruhl, J.H., Festa, V., Prosser, G., Langone, A., 2008. Multiple injections of
758 magmas along a Hercynian mid-crustal shear zone (Sila Massif, Calabria, Italy). Journal of
759 Structural Geology 30, 1202–1217.

760 Lister, G.S., Forster, M.A., Rawling, T.J., 2001. Episodicity during orogenesis. In: Miller, J.A., Holdsworth,
761 R.E., Buick, J.S., Hand, M. (Eds.), Continental Reactivation and Reworking. Geological Society,
762 London, Special Publications 184, 89–113.

763 Maino, M., Casini, L., Ceriani, A., Decarlis, A., Di Giulio, A., Seno, S., Setti, M., Stuart, F., 2015. Dating
764 shallow thrusts with zircon (U-Th)/He thermochronometry —The shear heating connection,
765 Geology 43, 495-498.

766 Maino, M., Dallagiovanna, G., Dobson, K., Gaggero, L., Persano, C. Seno, S., Stuart, F.M., 2012. Testing
767 models of orogen exhumation using zircon (U–Th)/He thermochronology: insight from the
768 Ligurian Alps, Northern Italy. Tectonophysics 560–561, 84–93.

769 Maino, M., Gaggero, L., Langone, A., Seno, S., Fanning, M., 2018. Cambro-Silurian magmatism at the
770 northern Gondwana margin (Penninic basement of the Ligurian Alps). Geoscience Frontiers,
771 doi.org/10.1016/j.gsf.2018.01.003.

772 Maino, M., Seno, S., 2016. The thrust zone of the Ligurian Penninic basal contact (Monte Frontè,
773 Ligurian Alps, Italy). Journal of Maps 12, 341-351.

774 Malusà, M.G., Faccenna, C., Baldwin, S.L., Fitzgerald, P.G., Rossetti, F., Balestrieri, M.L., Danisık, M.,
775 Ellero, A. Ottria, G., Piromallo, C., 2015. Contrasting styles of (U)HP rock exhumation along the
776 Cenozoic Adria-Europe plate boundary (Western Alps, Calabria, Corsica), Geochemistry,
777 Geophysics, Geosystems 16, 1786–1824.

778 Mameli, P., Mongelli, G., Oggiano, G., Dinelli, E., 2007. Geological, geochemical and mineralogical
779 features of some bauxite deposits from Nurra (Western Sardinia, Italy): insights on conditions of
780 formation and parental affinity. International Journal of Earth Sciences (Geologische Rundschau)
781 96, 887–902.

782 Marroni, M., Meneghini, F. Pandolfi, L., 2010. Anatomy of the Ligure-Piemontese subduction system:
783 evidence from Late Cretaceous–middle Eocene convergent margin deposits in the Northern
784 Apennines, Italy. International Geology Review 52, 1160-1192.

785 Marroni, M., Meneghini, F., Pandolfi, L., 2017. A Revised Subduction Inception Model to Explain the
786 Late Cretaceous, Double-Vergent Orogen in the Precollisional Western Tethys: Evidence From the
787 Northern Apennines. Tectonics 36 (10), 2227-2249.

788 Marroni, M., Molli, G., Ottria, G., Pandolfi, L., 2001. Tectono-sedimentary evolution of the External
789 Liguride units (northern Apennine, Italy): From rifting to convergence history of a fossil ocean-
790 continent transition zone. Geodinamica Acta 14, 307-320.

791 Marroni, M., Pandolfi, L., 2007. The architecture of an incipient oceanic basin: a tentative
792 reconstruction of the Jurassic Liguria-Piemonte basin along the Northern Apennines–Alpine

Corsica transect. International Journal of Earth Sciences (Geologische Rundschau) 96 (6), 1059-1078.

Mattern, F., 2005, Ancient sand-rich submarine fans: depositional systems, models, identification, and analysis. Earth-Science Reviews 70, 167-202

McCann, T., Arbues, P., 2012. Deep-marine sandstone provenance, Ainsa Basin, Southern Pyrenees, Spain. Zeitschrift der deutschen Geowissenschaften 22, 185-201.

McCann, T., Timmermann, M.J., Krzywiec, P., Lopez-Gomez, J., Wetzel, A., Krawczyk, C.M., Rieke, H., Lamarche, J., 2006. Post-Variscan (end Carboniferous-Early Permian) basin evolution in Western and Central Europe. In: Gee, D.G., Stephenson, R.A. (Eds.), European Lithosphere Dynamics, Geological Society, London, Memoirs 32, pp. 355-388.

Meinhold, G., Morton, A.C., Avigad, D., 2013. New insights into peri-Gondwana paleogeography and the Gondwana super-fan system from detrital zircon U–Pb ages. Gondwana Research 23, 661–665.

Ménot, R.-P., von Raumer, J.P., Bognadoff, S., Vivier, G., 1994. Variscan basement of the Western Alps: the External Crystalline Massifs. In: Keppie, J.D. (Ed.), Pre-Mesozoic Geology in France and related areas, Springer Verlag Berlin, Heidelberg, pp. 458-466.

Michard, A., Martinotti, G., 2002. The Eocene unconformity of the Briançonnais domain in the French—Italian Alps, revisited (Marguareis massif, Cuneo); a hint for a Late Cretaceous—Middle Eocene frontal bulge setting. Geodinamica Acta 15, 5-6.

Molli, G., 2008. Northern Apennine – Corsica orogenic system: an updated overview. In: Siegesmund, S., Fügenschuh, B., Froitzheim, N. (Eds.), Tectonic Aspects of the Alpine–Dinaride–Carpathian System, Geological Society of London, Special Publication 298, pp. 413-442.Molli, G., Malavieille, J., 2011. Orogenic processes and the Corsica/Apennines geodynamic evolution: insights from Taiwan. International Journal of Earth Sciences (Geologische Rundschau) 100, 1207-1224.

817 Mueller, P., Patacci, M., Di Giulio, A., 2017. Hybrid event beds in the proximal to distal extensive lobe
818 domain of the coarse-grained and sand-rich Bordighera turbidite system (NW Italy). Marine and
819 Petroleum Geology 86, 908–931.

820 Müntener, O., Hermann, J., 2001. The role of lower crust and continental upper mantle during
821 formation of non-volcanic passive margins: Evidence from the Alps. In: Wilson, R.C.L., Whitmarsh,
822 R.B., Taylor, B., Froitzheim, N. (Eds.). Non-Volcanic Rifting of Continental Margins: Evidence from
823 Land and Sea, Geological Sociecty of London, Special Publications 187, 267–288.

824 Najman, Y., 2006. The detrital record of orogenesis: a review of approaches and techniques used in
825 the Himalayan sedimentary basins. Earth Science Reviews 74, 1-72.

826 Oggiano, G., Gaggero, L., Funedda, A., Buzzi, L., Tiepolo, M., 2010. Multiple early Paleozoic volcanic
827 events at the northern Gondwana margin: U–Pb age evidence from the Southern Variscan branch
828 (Sardinia, Italy). Gondwana Research 17, 44-58.

829 Palomares, M., Arribas, J., 1993, Modern stream sands from compound crystalline sources:
830 Composition and sand generation index. Geological Society of America Special Paper 284, 313-
831 322.

832 Pandolfi, L., 1996. Le arenarie del M. Gottero nella sezione di punta Mesco (Campaniano Sup.-
833 Paleocene inf., Appennino settentrionale): analisi stratigrafica e petrografica della parte
834 prossimale di un sistema torbiditico. Atti Società Toscana Scienze Naturali, Memorie A 103, 197-
835 208.

836 Pandolfi, L., Marroni, M., Malasoma, A., 2016. Stratigraphic and structural features of the Bas-Ostriconi
837 unit (Corsica): paleogeographic implications. Compte Rendus Geoscience 348 (8), 630-640.

838 Paquette, J.-L., Ménot, R.-P., Pin, C., Orsini, J.-B., 2003. Episodic short-lived granitic pulses in a post-
839 collisional setting: evidence from precise U-Pb zircon dating through a crustal cross-section in
840 Corsica, Chemical Geology 198, 1-20.

841 Pavanetto, P., Funedda, A., Northrup, C.J., Schmitz, M., Crowley, J., Loi, A., 2012. Structure and U–Pb
842 zircon geochronology in the Variscan foreland of SW Sardinia, Italy. Geological Journal 47, 426-
843 445.

844 Pettijohn, F.J., 1975. Sedimentary rocks (third edition). Harper and Row, New York.

845 Puigdefabregas, C., Souquet, P., 1986. Tecto-sedimentary cycles and depositional sequences of the
846 Mesozoic and Tertiary from the Pyrenees. Tectonophysics 129, 173–203.

847 Quick, J.E., Sinigoi, S., Peressini, G., Demarchi, G., Wooden, J.L., Sbisà, A., 2009, Magmatic plumbing of
848 a large Permian caldera exposed to a depth of 25 km. Geology 37, 603–606.

849 Ronca, S., Del Moro, A., Traversa, G., 1999. Geochronology, Sr-Nd isotope geochemistry and petrology
850 of late-Hercynian dyke magmatism from Sarrabus (SE Sardinia). Periodico di Mineralogia 68, 231-
851 260.

852 Rosenbaum, G., Lister, G.S., 2005. The Western Alps from the Jurassic to Oligocene: spatio-temporal
853 constraints and evolutionary reconstructions. Earth-Science Reviews 69, 281-306.

854 Rossi, P., Oggiano, G., Cocherie, A., 2009. A restored section of the ‘‘southern Variscan realm’’ across
855 the Corsica–Sardinia microcontinent. Compte Rendus Geoscience 341, 224-238.

856 Rowan, M.G., 1990. The Upper Cretaceous Helminthoid Flysch of the Northern Apennines and
857 Maritime Alps: Correlation and Provenance. Ofioliti 15, 305-326.

858 Rubatto, D., Regis, D., Hermann, J., Boston, K., Engi, M., Beltrando, M., McAlpine, S.R.B., 2011. Yo-yo
859 subduction recorded by accessory minerals in the Italian Western Alps, Nature Geoscience 4, 338–
860 342.

861 Rubatto, D., Schaltegger, U., Lombardo, B., Colombo, F., Compagnoni, R., 2001. Complex Palaeozoic
862 magmatic and metamorphic evolution in the Argentera Massif (Western Alps) resolved with U–
863 Pb dating. Swiss Bulletin of Mineralogy and Petrology 81, 213–228.

Sagri, M., 1980. Le Arenarie di Bordighera: una conoide sottomarina nel bacino di sedimentazione dei Flysch ad Elmintoidi di San Remo (Cretaceo Superiore, Liguria Occidentale). Bollettino della Società Geologica Italiana 98-99, 205-226.

Sagri, M., 1984. Litologia, stratimetria e sedimentologia delle torbiditi di piana di bacino del Flysch di San Remo (Cretaceo superiore, Liguria occidentale). Memorie della Società Geologica Italiana 28, 577-586.

Sagri, M., Marri, C., 1980. Paleobatimetria e ambienti di deposizione delle unità torbiditiche Cretaceo-Superiori dell'Appennino settentrionale. Memorie della Società Geologica Italiana 21, 231-240.

Sandrone, R., Cadoppi, P., Sacchi, R., Vialon, P., 1993. The Dora-Maira Massif. In: von Raumer, J.F., Neubauer, F. (Eds.), Pre-Mesozoic Geology in the Alps. Springer, Berlin, Heidelberg, pp. 317-325.

Satkoski, A.M., Wilkinson, B.H., Hietpas, J.H., Samson, S.D., 2013. Likeness among detrital zircon populations – an approach to the comparison of age frequency data in time and space. Geological Society of America Bulletin 125, 1783–1799.

Saylor, J.E., Sundell, K.E., 2016. Quantifying comparison of large detrital geochronology data sets, Geosphere 12, 203-220, doi: https://doi.org/10.1130/GES01237.1

Schmid, M.S., Fügenschuh B., Kissling E., Schuster R., 2004. Tectonic map and overall architecture of the Alpine orogen. Eclogae Geologicae Helvetiae 97, 93–117.

Schmid, S.M., Pfiffner, O.A., Froitzheim, N., Schönborn, G., Kissling, E., 1996. Geophysical-geological transect and tectonic evolution of the Swiss-Italian Alps. Tectonics 15, 1036-1064.

Seno, S., Dallagiovanna, G., Vanossi, M., 2005. Pre-Piedmont and Piedmont-Ligurian nappes in the central sector of the Ligurian Alps: a possible pathway for their superposition on to the inner Briançonnais units. Bollettino della Società Geologica Italiana 124, 455-464.

Sestini, G., 1970. Sedimentation of the late geosynclinal stage. Sedimentary Geology 4, 445–479.

887 Shanmugam, G., Moiola, R.J., 1988, Submarine fans: characteristics, models, classification, and
888 reservoir potential. Earth-Science Reviews 24, 383–428.

889 Stampfli, G.M., von Raumer, J., Wilhelm, C., 2012. The distribution of Gondwana-derived terranes in
890 the Early Paleozoic. In: Gutiérrez-Marco, J.C., Rábano, I., García-Bellido, D. (Eds.), Ordovician of
891 the World. Cuadernos del Museo Geominero 14. Instituto Geológico y Minero de España, Madrid,
892 pp. 567-574.

893 Stockmal, G.S., Beaumont, C., Boutilier, R., 1987. Geodynamic models of Convergent Margin Tectonics:
894 Transition from Rifted Margin to Overthrust Belt and Consequences for Foreland basement
895 development. AAPG Bulletin 70 (2), 181-190.

896 Thomas, M.F.H., Bodin, S., Redfern, J., 2010. Comment on `European provenance of the Numidian
897 Flysch in northern Tunisia´ by Fildes et al. (2010). Terra Nova 22, 501-503.

898 Traversa, G., Ronca, S., Del Moro, A., Pasquali, C., Buraglini, N., Barabino, G., 2003. Late to post-
899 Hercynian dyke activity in the Sardinia-Corsica Domain: A transition from orogenic calcalkaline to
900 anorogenic alkaline magmatism. Bollettino della Società Geologica Italiana, Special Volume 2,
901 131-152.

902 Valloni, R., Zuffa, G.G., 1984. Provenance changes for arenaceous formations of the northern
903 Apennines, Italy. Geological Society of America Bulletin, 95, 1035–1039.

904 van de Kamp, P.C., Leake, B.E., 1995. Petrology and geochemistry of siliciclastic rocks of mixed
905 feldspathic and ophiolitic provenance in the Northern Apennines, Italy. Chemical Geology 122, 1-
906 20.

907 Vanossi, M., 1965. Studio sedimentologico del Flysch ad Elmintoidi della Valle Argentina (Liguria
908 occidentale). Atti Istituto della Geologia Pavia 16, 36-71.

909 Vanossi, M., Cortesogno, L., Galbiati, B., Messiga, B., Piccardo, G., Vannucci, R., 1986. Geologia delle
910 Alpi liguri: dati, problemi, ipotesi. Memorie della Società Geologica Italiana 28, 5–75.

911 Viti, M., Mantovani, E., Babbucci, D., Tamburelli, C., 2009, Generation of Trench-Arc-Back Arc Systems
912 in the Western Mediterranean Region Driven by Plate Convergence. Bollettino Della Societa
913 Geologica Italiana (Italian Journal of Geosciences) 128, 89-106.

914 von Raumer, J.F., Stampfli, G.M., Arenas, R., Sánchez Martínez, S., 2014. Ediacaran to Cambrian oceanic
915 rocks of the Gondwana margin and their tectonic interpretation. International Journal of Earth
916 Sciences (Geologische Rundschau) 104, 1107–1121.

917 von Raumer, J.F., Stampfli, G.M., Borel, G., Bussy, F., 2002. Organization of pre-Variscan basement area
918 at the north-Gondwanan margin. International Journal of Earth Sciences (Geologische Rundschau)
919 91, 35-52.

920 von Raumer, J.F., Stampfli, G.A., Bussy, F., 2003. Gondwana-derived microcontinents-the constituents
921 of the Variscan and Alpine collisional orogens. Tectonophysics 365, 7-22.

922 Vermeesch, P., 2012. On the visualisation of detrital age distributions. Chemical Geology 312–313,
923 190–194.

924 Wildi, W., 1985. Heavy mineral distribution and dispersal pattern in penninic and ligurian flysch basins
925 (Alps, northern Apennines). Giornale di Geologia 47, 77-99.

926 Wildi, W., 1987. Les regions sources du materiel terrigene dans les flyschs alpins. Géologie Alpine: Le
927 detritisme dans le Sud-Est de la France 13, 379-388.

928 Williams, I.S., Fiannacca, P., Cirrincione, R., Pezzino, A., 2012. Peri-Gondwanian origin and early
929 geodynamic history of NE Sicily: a zircon tale from the basement of the Peloritani Mountains.
930 Gondwana Research 22, 855–865.

931 Zhang, J., Dai, J. Quian, X., Ge, Y., Wang, C., 2016. Sedimentology, provenance and geochronology of
932 the Miocene Qiuwu Formation: Implication for the uplift history of Southern Tibet. Geoscience
933 Frontiers 8, 823-839.

934

935 **Figure captions:**

936 **Fig. 1.** Simplified geological map of the Western Alps denoting the main paleogeographic units.
937 Modified after Schmid et al. (2004) and Bousquet et al. (2008). Location of the study area is indicated
938 in the black rectangle.

939

940 **Fig. 2. (**A) Geological map of the study area (box in Fig. 1). Modified after Lanteaume et al. (1990) and
941 Di Giulio and Galbiati (1991). Rose diagram of palaocurrent measurements (n = 107) for the Bordighera
942 Sandstone delineates the predominantly NNE-directed orientation of sediment flux. (B) Tentative
943 chronostratigraphic framework of the San Remo-Monte-Saccarello Unit and approximate stratigraphic
944 positions of the studied detrital zircon samples. Modified after Cobianchi et al. (1991), Galbiati and
945 Cobianchi (1997) and Giammarino et al. (2010).

946

947 **Fig.3.** Outcrop examples of the stratigraphic members of the San Remo-Monte Saccarello Unit. (A)
948 Sample location of the lowermost terrigenous lithozone of the San Bartolomeo Fm. (variegated shales
949 with locally intercalated very fine-grained sandstones) at the type location north of the town of
950 “Badalucco” (see also Fig. 2A). GPS 43°55'15.47"N, 7°50'31.79"E. (B) Sample location of the uppermost
951 analyzed terrigenous lithozone of the San Bartolomeo Fm. (fine- to medium quartzarenites that exhibit
952 normal grading) in the Valle Argentina. GPS 43°55'32.57"N, 7°50'35.75"E; (C) Panoramic view of the
953 San Remo-Monte Saccarello Unit comprising the conformably superimposing San Bartolomeo Fm.
954 (SBF), the Bordighera Sandstone (BGS) and the calcareous San Remo Flysch (SRF) cropping out in an
955 anticlinal structure at sample location “Monte Frontè”. Sampling location: GPS 44° 2'44.45"N,
956 7°45'10.48"E. D) Outcrop image of the coarse-clastic Bordighera Sandstone at the distalmost sample
957 location “Cima di Velega”. GPS 44° 7'46.55"N, 7°40'33.45"E. Note that strata are overturned.

958

Fig. 4. Representative thin section microphotographs for samples of the San Bartolomeo Fm. (SBF; A-C) and the Bordighera Sandstone (BGS; D-I). (A) Typical appearance of relatively well-sorted, tightly packed SBF samples. Note the textural and compositional maturity of the sandstone. (B) Characteristic quartz-dominated nature of fine-grained SBF thin-sections. Note the sub-rounded to occasionally rounded grain shapes. (C) Uppermost SBF sample illustrating lithic fragment examples: chert fragment (Ls) and volcanic fragment (Lv). (D) Characteristic poorly mature BGS sample, showing poor degree of sorting, angular grains and an arkosic composition. (E) Typical constituents of the coarse detritus represented by monocrystalline quartz (Qm), alkali feldspar (K-F) and mica (m). (F) Typical alteration of plagioclase in association with monocrystalline quartz in tightly packed framework almost devoid of matrix. (G) Examples of lithic fragments: arkosic fragment (Ls) and volcanic fragment (Lv) in association with Qm and plagioclase (Plg). Note the abundant pinkish calcite cement (c_c). (H) Representative arkosic composition comprising quartz and feldspars (in granitic fragment), and low-grade metamorphic lithic grain (Lm). (I) Fine- and microcrystalline polycrystalline quartz grains (Qp) in metamorphic fragment in association with a chert sedimentary lithic fragment (Ls).

Fig. 5. Sandstone modal compositions of the San Bartolomeo Fm. and the Bordighera Sandstone. (A) QtFL modal analysis (cf., Dickinson et al., 1983) and (B) QmPK modal analysis ternary plots (cf., Dickinson and Suczek, 1979). Note the consistent dominance of K-feldspar over plagioclase in all the studied samples in the QmPK plots.

Fig. 6. Maturity indexes (whisker plots) for samples from the three analyzed sections. Monte Frontè = medial domain of the Bordighera Sandstone; Cima di Velega = distalmost domain of the Bordighera Sandstone.

983 **Fig. 7.** Cathodoluminescence images of representative detrital zircon grains from samples SBF_1 (A),
984 SBF_4 (B), MF_1 (C), CdV_1 (D) and CdV_3 (E).

985

986 **Fig. 8.** Qualitative comparison of detrital age frequency distributions (probability density plots) of the
987 analyzed samples for A) the time interval from 0-3500 Ma and B) for the time interval from 200-1200
988 Ma. Geological time-scale according to the International Commission on Stratigraphy.

989

990 **Fig. 9. (**A) Qualitative confrontation of the detrital age spectra (cumulative distribution functions) for
991 the time span from 0-3500 Ma and (B) Statistical evaluation of similarity (K-S test p-values) between
992 the detrital samples cumulative distribution functions. Green-shaded boxes indicate p-values > 0.05,
993 whereas red-shaded boxes indicate that confrontations did not pass the threshold value of 0.05.

994

995 **Fig. 10.** Histograms (bin size 5 Ma) and synthetic probability density curves of all concordant ages of
996 samples of the Bordighera Sandstone (BGS) and the San Bartolomeo Fm. (SBF): (A) Age spectrum from
997 200 Ma to 800 Ma; (B) Age spectrum from 200 to 450 Ma.

998

999 **Fig. 11.** Kernel Density Estimation (KDE) plots of detrital zircon ages (200-1200 Ma) of the San
1000 Bartolomeo Fm. and the Bordighera Sandstone and of some published detrital zircon age data from
1001 Corsican (?) para-autochthonous flysch units (Eocene Annunciata flysch; samples 11CO68 and 11CO87
1002 from Lin et al. (2017) and from the allochthonous successions of the Piedmont Nappe (Late Cretaceous
1003 Narbinco Fm. and Coniacian-Maastrichtian Tralonca Fm.) and the Albian-Cenomanian "Lydienne
1004 flysch" of the Balagne Nappe (Lin et al., 2018).

1005

Fig. 12. Models for the evolution of the provenance of the investigated successions (not to scale), illustrating the effect of the inferred craton-ward (i.e., NNW-directed) shift of the flexural bulge hinge line. (A) During the Hauterivian to Santonian the flexural bulge was located in the extensive shelfal area of the distal European margin. (B) During the Campanian to Maastrichtian the flexural bulge arrived in the more proximal part of the margin. Resultant rapid uplift of crustal blocks promoted rapid sedimentation of the first-cycle Bordighera Sandstone arkoses which were shed into the trench without significant surface processes (physical and chemical) coming into effect.

1028 Fig. 1

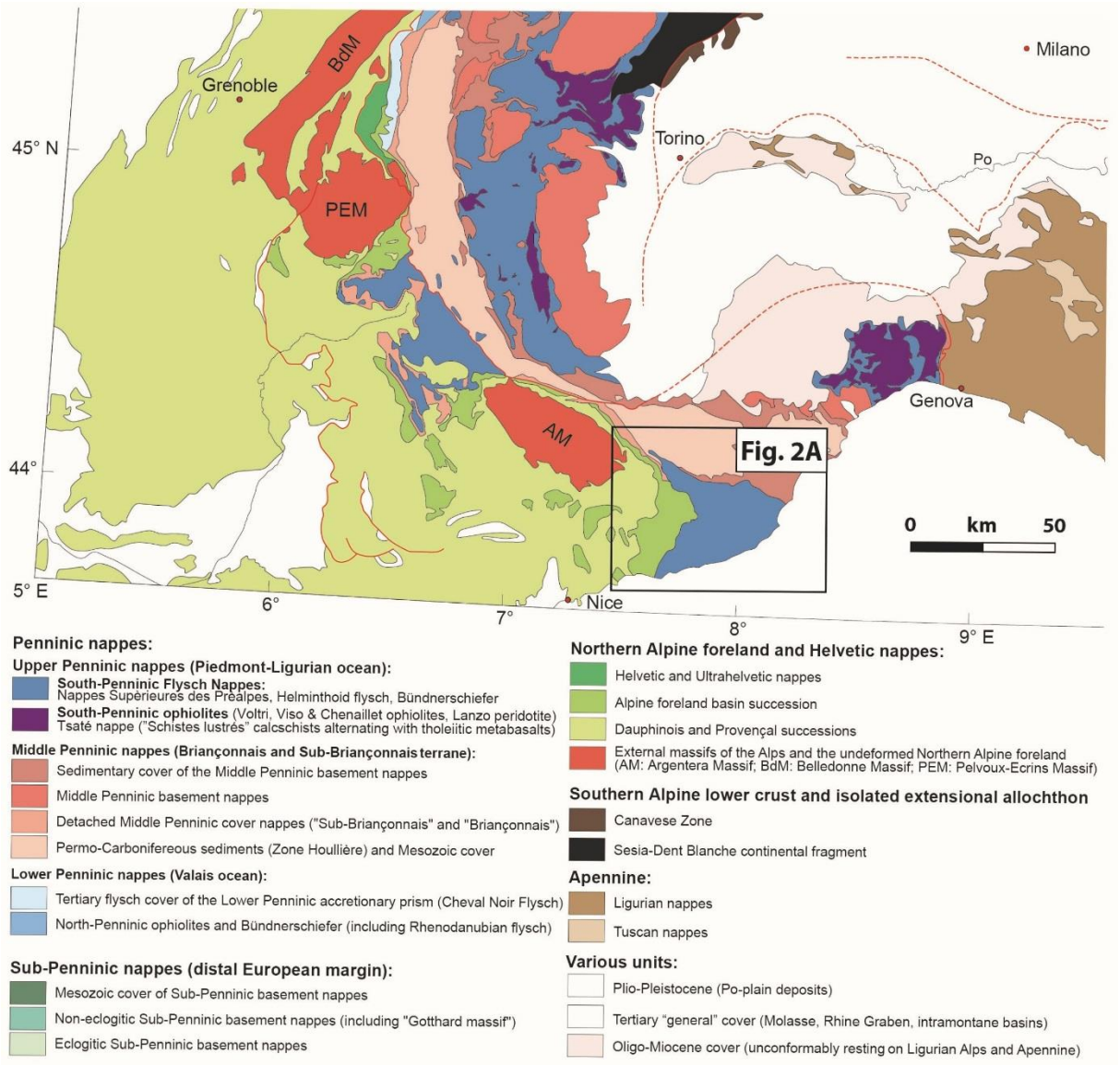

1029

1030

1031

1032

1033

1034

1035

1036 Fig. 2

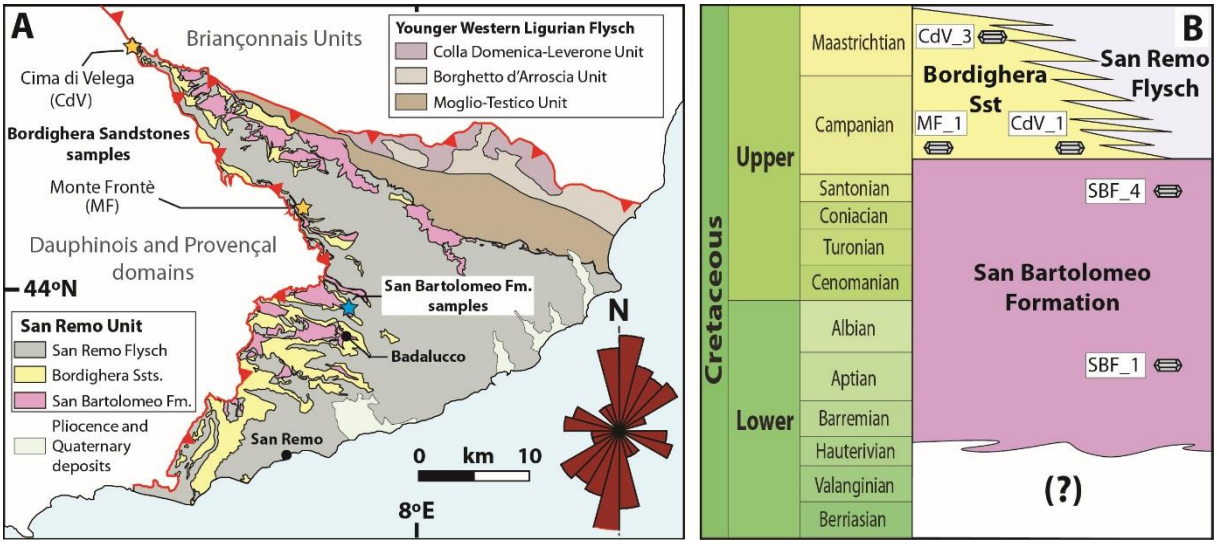

1037

1038

1039

1040

1041

1042

1043

1044

1045

1046

1047

1048

1049

1050

1051 Fig. 3

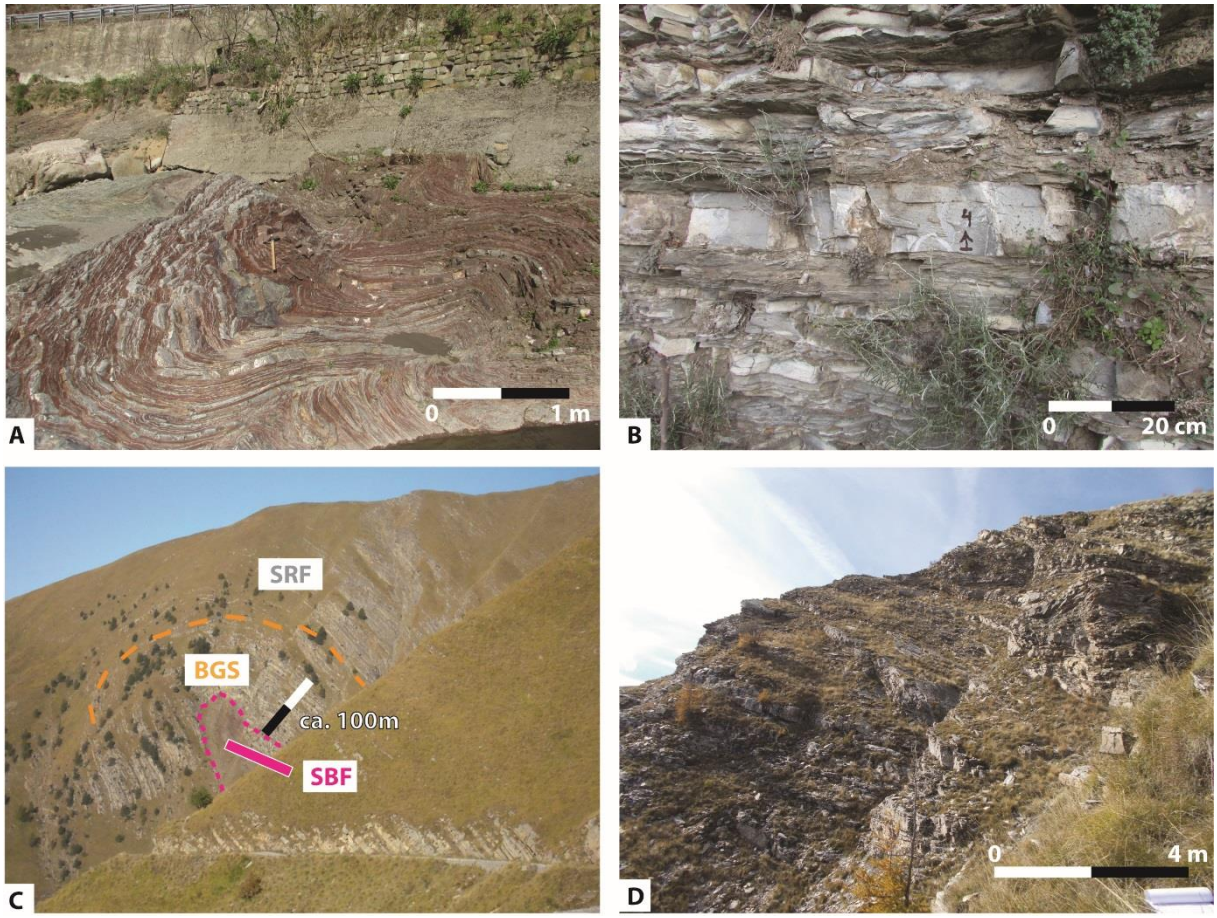

1052

1053

1054

1055

1056

1057

1058

1059

1060

1061

Fig. 4

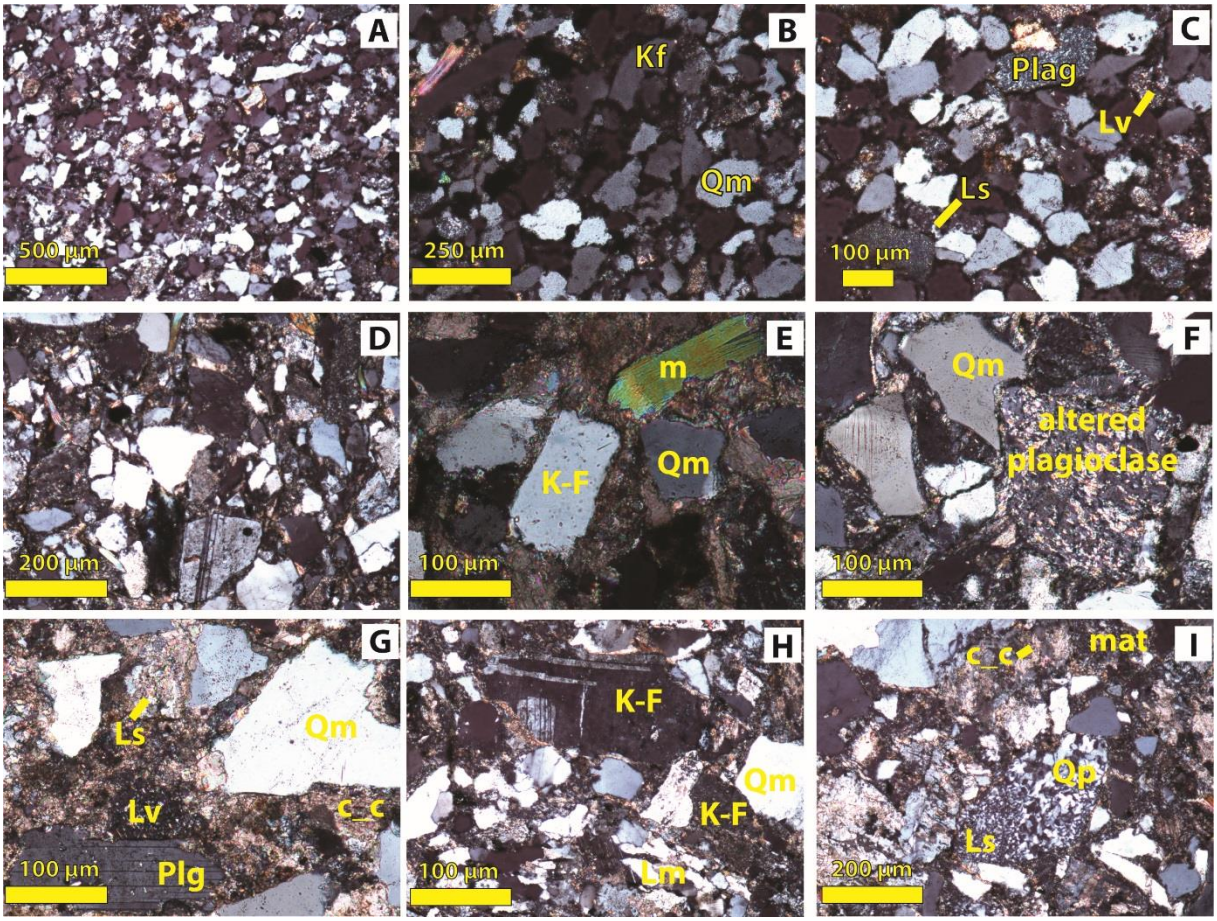
A
500 µm
B
Kf
Qm
250 µm
C
Plag
Lv
Ls
100 µm
D
200 µm
E
m
K-F
Qm
100 µm
F
Qm
altered
plagioclase
100 µm
G
Ls
Qm
Lv
c_c
100 µm
Plg
H
K-F
Qm
K-F
100 µm
Lm
I
c_c
mat
Qp
Ls
200 µm

1073 Fig. 5

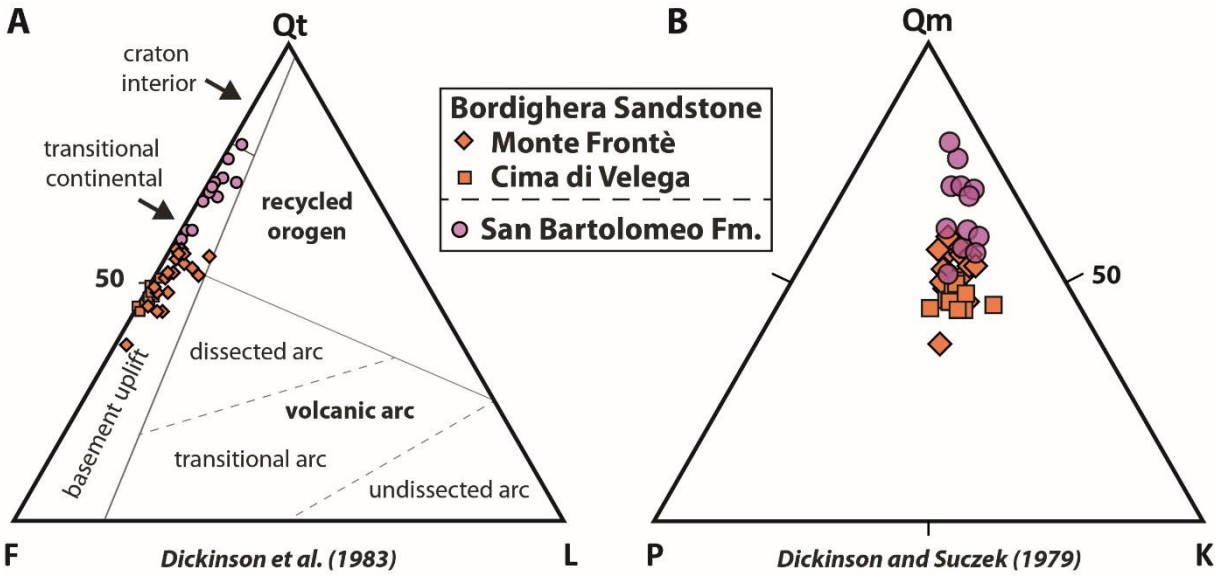

1074

1075

1076

1077

1078

1079

1080

1081

1082

1083

1084

1085

1086

1087

1088 Fig. 6

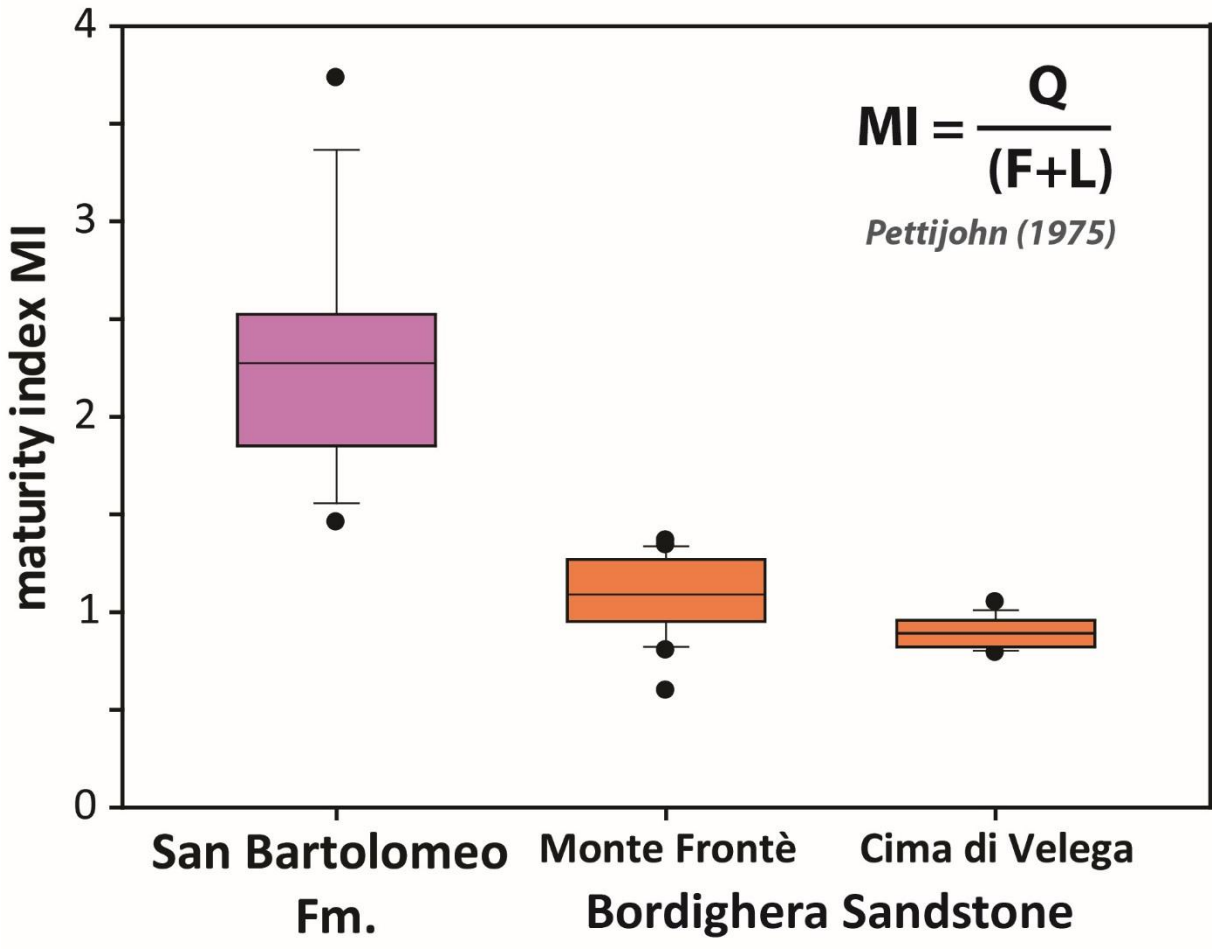

1089

1090

1091

1092

1093

1094

1095

1096

1097

1098

Fig. 7

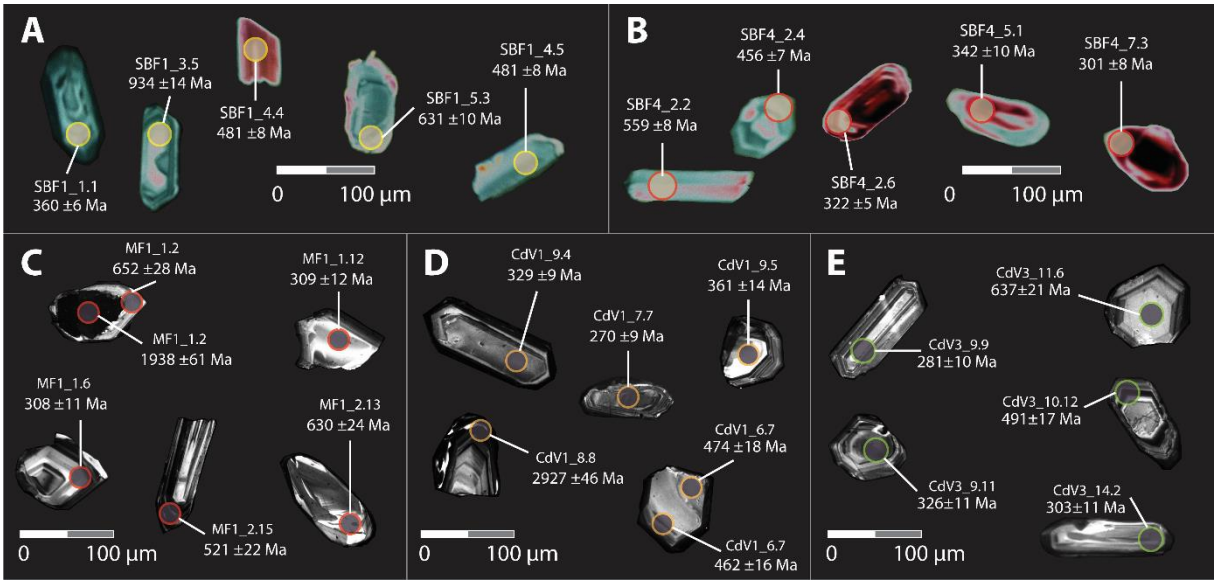
A
SBF1_1.1
360 ±6 Ma
SBF1_3.5
934 ±14 Ma
SBF1_4.4
481 ±8 Ma
SBF1_5.3
631 ±10 Ma
SBF1_4.5
481 ±8 Ma
0
100 µm
B
SBF4_2.2
559 ±8 Ma
SBF4_2.4
456 ±7 Ma
SBF4_2.6
322 ±5 Ma
SBF4_5.1
342 ±10 Ma
SBF4_7.3
301 ±8 Ma
0
100 µm
C
MF1_1.2
652 ±28 Ma
MF1_1.2
1938 ±61 Ma
MF1_1.12
309 ±12 Ma
MF1_1.6
308 ±11 Ma
MF1_2.13
630 ±24 Ma
MF1_2.15
521 ±22 Ma
0
100 µm
D
CdV1_9.4
329 ±9 Ma
CdV1_7.7
270 ±9 Ma
CdV1_9.5
361 ±14 Ma
CdV1_8.8
2927 ±46 Ma
CdV1_6.7
474 ±18 Ma
CdV1_6.7
462 ±16 Ma
0
100 µm
E
CdV3_11.6
637±21 Ma
CdV3_9.9
281±10 Ma
CdV3_10.12
491±17 Ma
CdV3_9.11
326±11 Ma
CdV3_14.2
303±11 Ma
0
100 µm

1114 Fig. 8

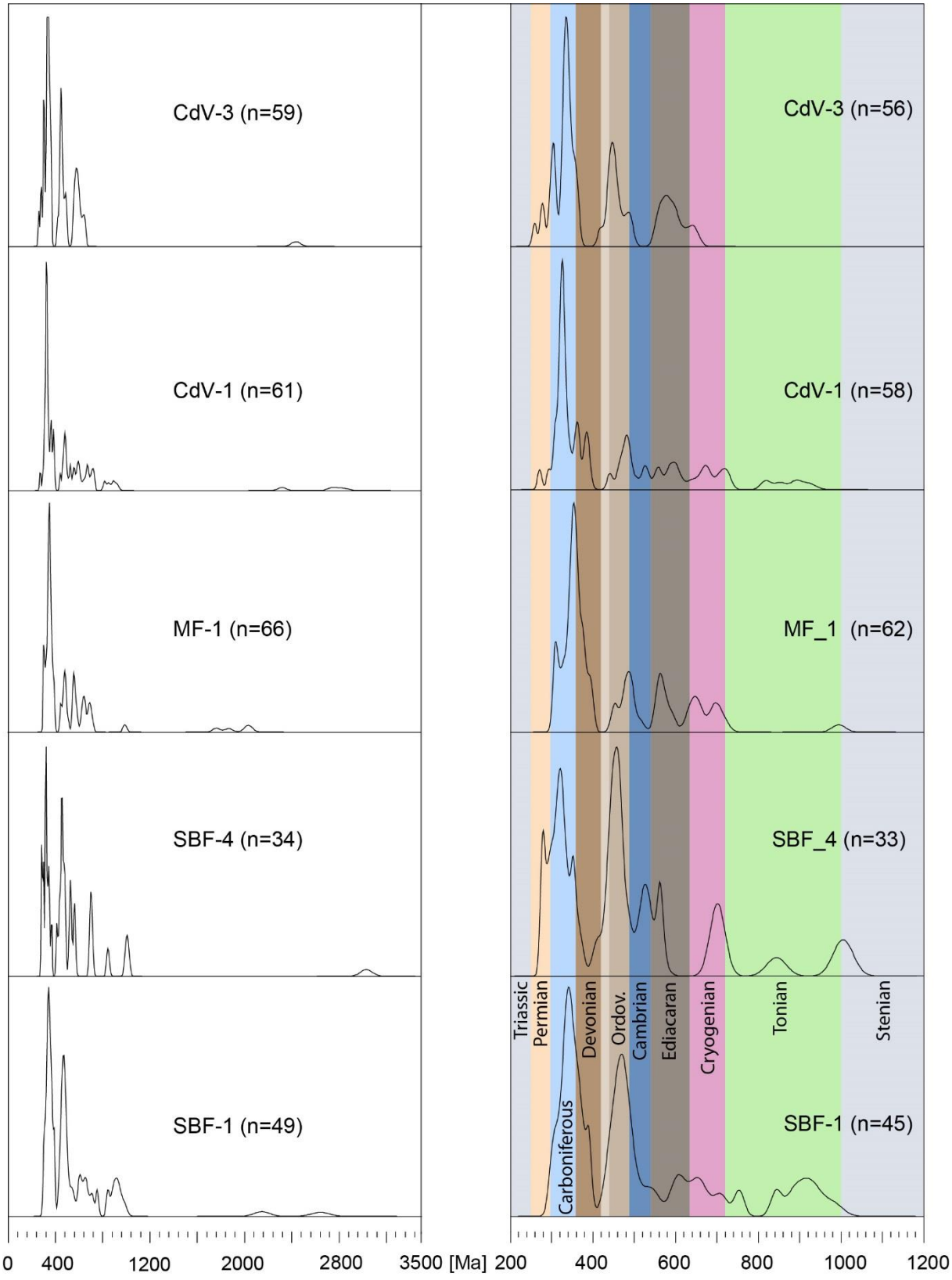

1115

1116

Fig. 9

A)

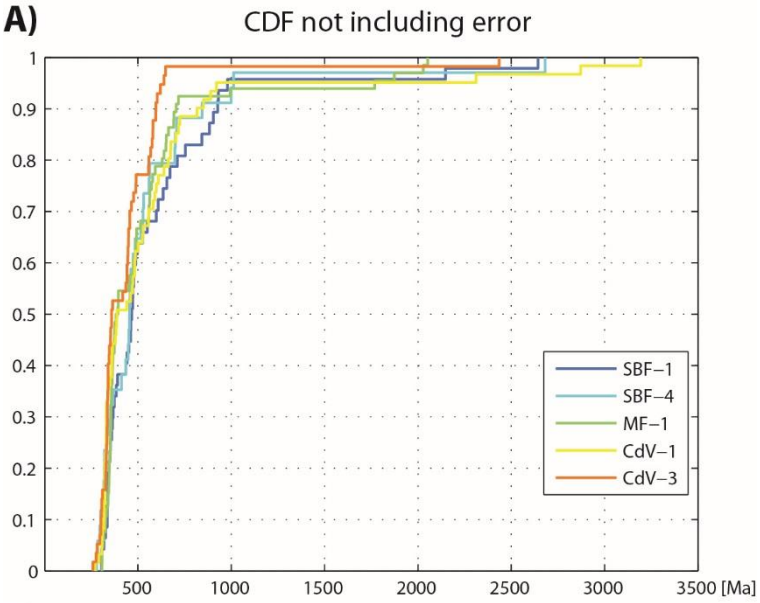

B)

K-S test p value					
	SBF-1	SBF-4	MF-1	CdV-1	CdV-3
SBF-1	1	0.506075	0.429343	0.073544	0.058132
SBF-4	0.506075	1	0.340518	0.63103	0.199757
MF-1	0.429343	0.340518	1	0.10868	0.033701
CdV-1	0.073544	0.63103	0.10868	1	0.186431
CdV-3	0.058132	0.199757	0.033701	0.186431	1

1128 Fig. 10

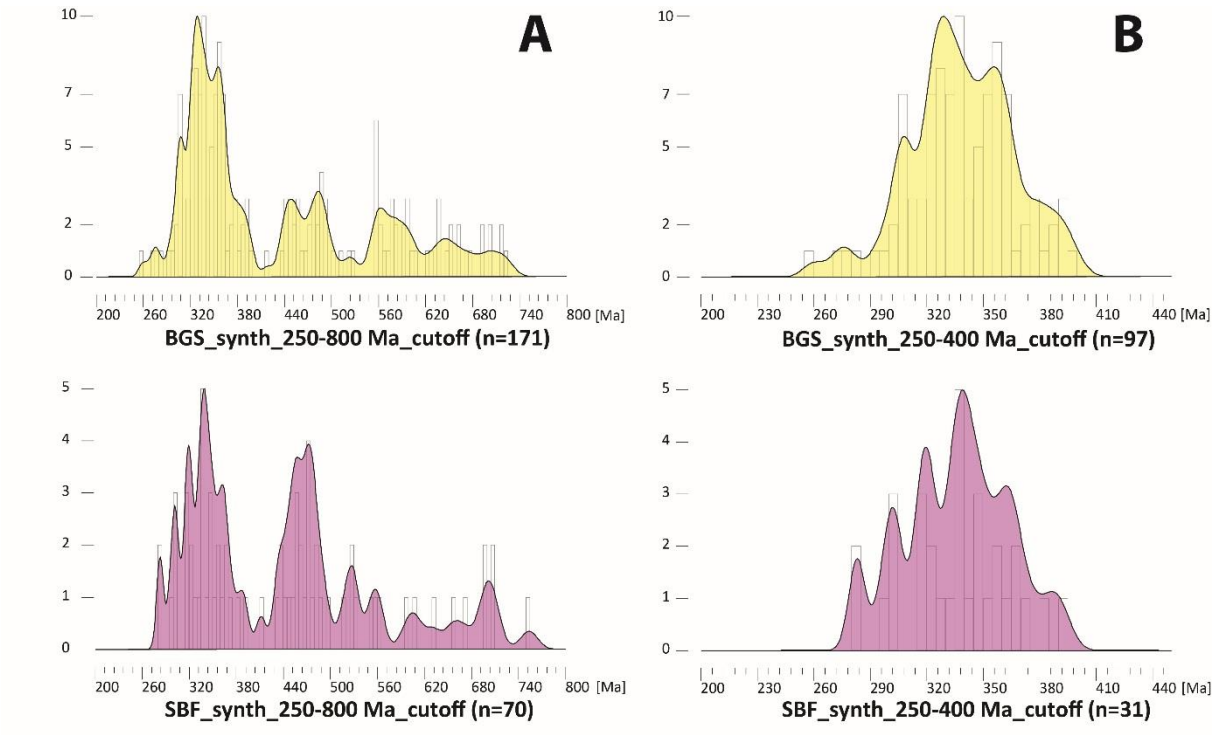

1129

1130

1131

1132

1133

1134

1135

1136

1137

1138

1139

1140

1141 Fig. 11

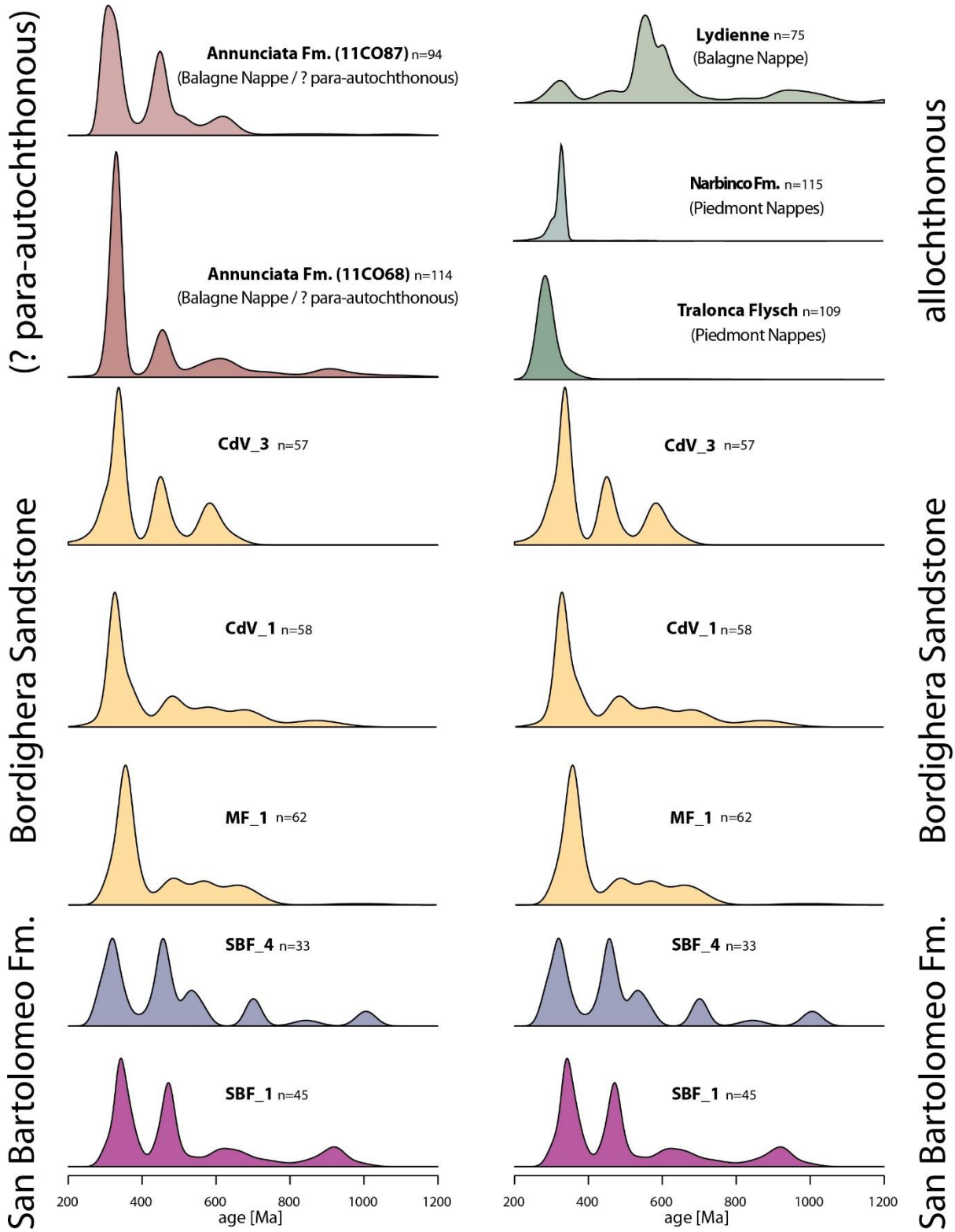

1142

1143

1144

1145 Fig. 12

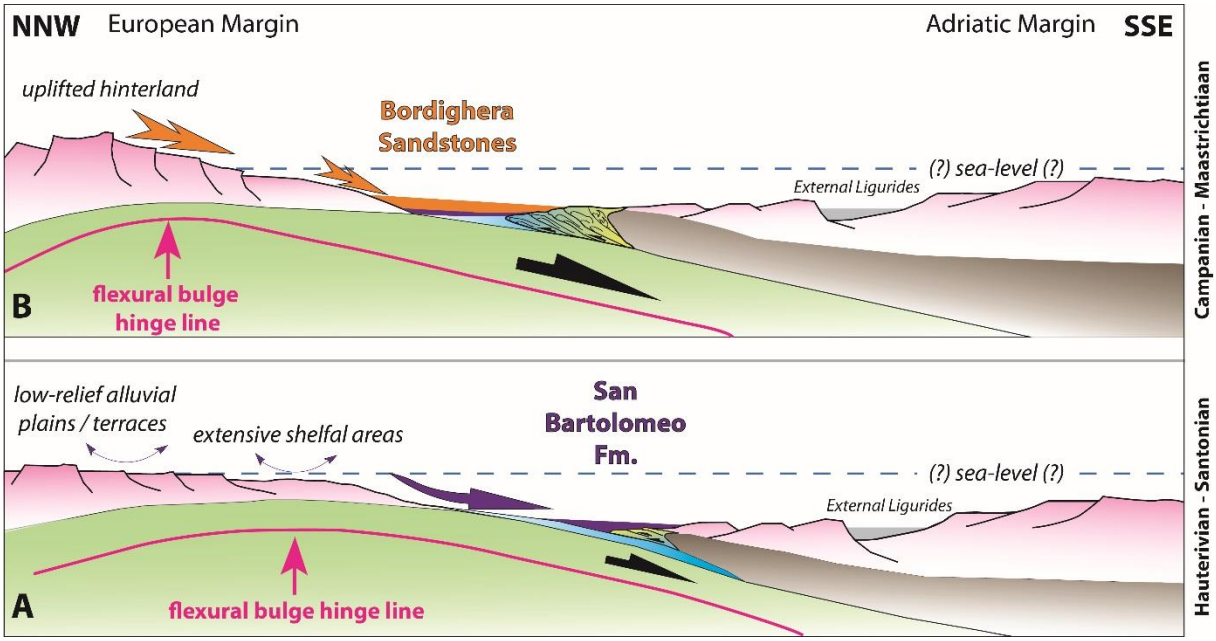

1146

1147